

Response to comments of reviewer #1

This study examined the source contributions to Arctic black carbon (BC) in 2010 using the Flexpart Lagrangian transport model version 10.1 equipped with a new aerosol wet removal scheme. They found that Arctic BC at the surface and high altitudes is sensitive to emissions in high latitude and mid-latitude regions, respectively. About half of Arctic surface BC comes from anthropogenic emissions in Russia and 40% of BC at high altitudes comes from anthropogenic emissions in East Asia. The results can contribute to the Arctic aerosol community and the method with the new wet deposition scheme can improve high latitude aerosol simulation with lagrangian models.

Response:

We appreciate the reviewer for the positive evaluations. The comments are truly helpful in improving the work. Each of the comments is responded as follows.

Major comment:

It is good to add more literatures using models in the revised manuscript. However, I still feel the description lacks of details. The authors listed many literatures in lines 79-92, but they did not give their result quantitatively. They stated that 'Although numerous studies have been performed, results regarding regional contributions of BC sources in the Arctic are still inconclusive.' I was expecting to see the differences of BC source contributions between this study and other studies and the possible causes of the differences, but they only showed the similarity between the Flexpart Lagrangian transport model and GEOS-Chem in the last part of the paper. I agree that using the new wet removal scheme can improve the aerosol simulation, but it should not be listed as the new method since that the scheme was introduced in this model in Grythe et al. (2017). The authors need to highlight the unique findings in the manuscript.

Response:

Taking the comments, we added quantitative results about estimated major source regions/sectors of BC in the Arctic by previous studies along with model types, settings, meteorology, emission inventories, etc., placed them in Table 1, and revised the context accordingly.

Regarding the simulations of BC in the Arctic, the treatment of wet-scavenging parameterizations is a key factor affecting the model performance. The new wet removal scheme of Flexpart v10 introduced by Grythe et al. (2017) was a big improvement of the model in this context comparing to its previous versions. To apply the new version model to study BC in the Arctic, is the new point of the study. Comparing to Arctic BC studies using Flexpart v9, such as by Stohl et al. (2013) and Winiget et al. (2019), we found that the contribution of gas flaring to Arctic BC simulated by Flexpart v10 is 22% higher using the same emission inventory. We also used an updated emission inventory about gas flaring for Russia by Huang et al. (2015), which was reported to be closer to the real situation. We have revised the manuscript to make such a purpose clearer, as follows.

In L87-89, we revised as “The treatment of wet-scavenging parameterizations is a key factor affecting the model performance, which determines the uncertainties related to BC particle removal (Kipling et al., 2013; Schacht et al., 2019; Q. Wang et al., 2014).”

In L96-108, the difference of Flexpart versions was placed as “The FLEXible PARTicle dispersion model (Flexpart) had been used to investigate the transport pathways and source contributions of BC in the Arctic (Stohl et al., 1998, 2006, 2013). Of Flexpart model up to version 9, wet removal was treated considering below-cloud and within-cloud scavenging processes (Hertel et al., 1995; McMahon and Denison, 1979), which depends on cloud liquid water content, precipitation rate and the depth of the cloud. However, clouds were parameterized based on relative humidity, clouds frequently extended to the surface and at times no clouds could be found in grid cells, with unrealistic precipitation (Grythe et al., 2017). Recently, version 10 of Flexpart had been developed in which cloud is differentiated into liquid, solid, and mixed phase, the cloud distribution is more consistent with the precipitation data (Grythe et al., 2017). This improvement in the cloud distribution and phase leads to a more realistic distribution of below-cloud and in-cloud scavenging events. In this study, we quantified region-separated sources of BC in the Arctic in 2010 by using Flexpart v10.1.”

Regarding the difference of current findings with those by previous versions of Flexpart, we newly evaluated the sectorial contributions (open biomass burning, residential burning, gas flaring, and others) to Arctic BC in Figure 5. Our results indicated that residential combustions are important sources of Arctic surface BC (36% in October–March), supporting those by Stohl et al. (2013). Meanwhile, we estimated a higher value of gas flaring source BC (annually 17.5 ng m^{-3} , 36% of total) than those by Stohl et al. (2013). Such a difference could be attributed to the model treatment of BC removal as well as the inventory differences.

Such comparisons were added in L305-322, as “On an annual basis, anthropogenic sources and open biomass burning emissions accounted for 82 % and 18 %, respectively, of total Arctic surface BC. In which, gas flaring and residential burning (including burning of fossil fuels and biofuels) are accounting for 36 % (28–57 % in October–March) and 15 % (13–25 % in October–March), respectively (Fig. 5a-b). Our results support Stohl et al. (2013) that residential combustion emissions, especially in winter are important sources of Arctic BC (Table 1). We estimated a contribution of gas flaring to Arctic surface BC of 17.5 ng m^{-3} (36% of total). In comparison, the value was estimated as 11.8 ng m^{-3} using an average Arctic surface BC of 28 ng m^{-3} and a fraction from gas flaring of 42 % evaluated by earlier versions of Flexpart (Stohl et al., 2013; Winiger et al., 2019). The different contribution could be partly attributed to the difference in gas flaring emission inventory. BC emission from gas flaring in Russia by Huang et al. (2015) was used in the current study, where total BC emission from gas flaring in Russia in 2010 was ca. 81.1 kilotonne, which was larger than the estimate of ca. 64.9 kilotonne by GAINS inventory (Klimont et al., 2017) used by Stohl et al. (2013). Moreover, Adopting ECLIPSEv5 inventory as was used by Winiger et al. (2019), we estimated that gas flaring was contributing 14.4 ng m^{-3} to Arctic surface BC using Flexpart v10.1, a value 22 % higher than those obtained using Flexpart v9. This difference could be attributed to the improvement of the wet-scavenging scheme by Flexpart v10.1”.

Newly added Figure 5:

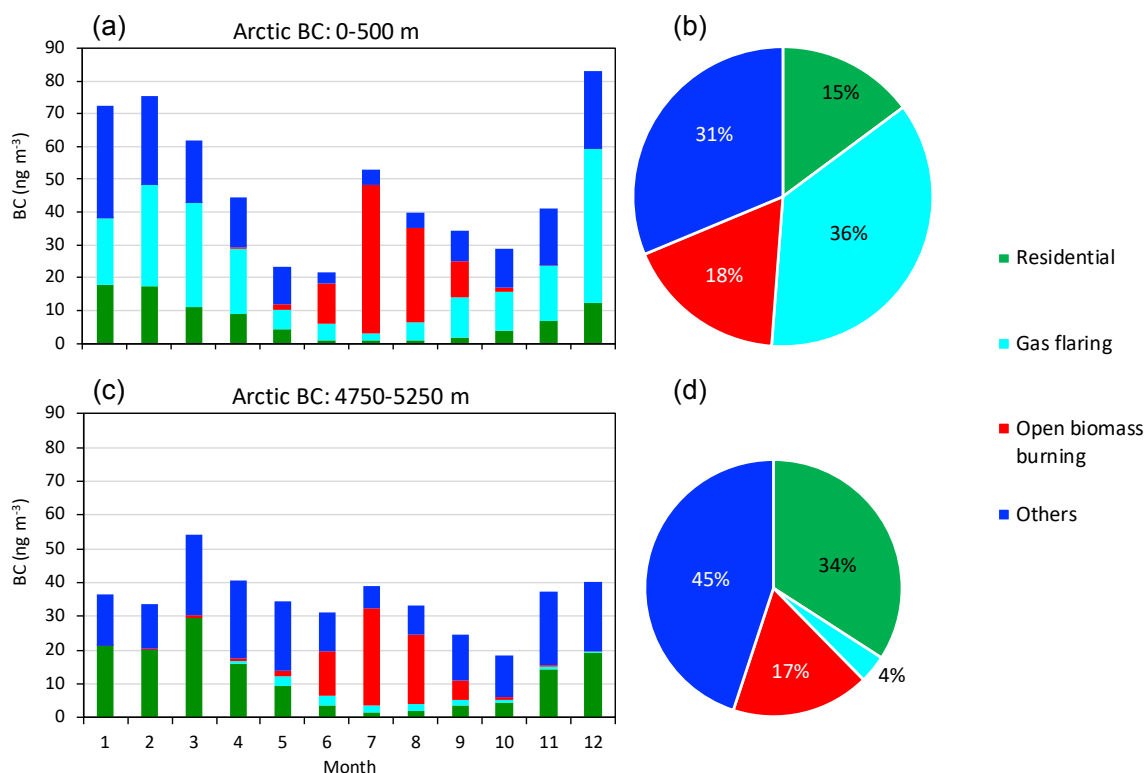


Figure 5. Sectorial contributions from residential combustion (including fossil fuel and biofuel combustions), gas flaring, open biomass burning and others (energy other than gas flaring, industry and transport) to (a) seasonal variations in Arctic surface BC, (b) annual mean Arctic surface BC, (c) seasonal variations in Arctic BC at high altitudes, and (d) annual mean of Arctic BC at high altitudes.

Specific comments:

Line 133: The Flexpart lagrangian transport model has some assumptions, like the hydrophilic BC. The uncertainties of the results related to the these assumption should be discussed.

Response:

Taking the comment, we added in the method section in L146-148 as “This may lead to an overestimation of BC removal and hence force underestimation of simulated BC concentration, especially of fossil fuel combustion sources where BC could be in the hydrophobic state for a few days.”, and in L227-230 as “The underestimation by Flexpart could also be partly contributed by the assumption that all particles are hydrophilic, where the BC scavenging could be overestimated. The corresponding uncertainties are larger in winter months, when there are more sources from fossil fuel combustion.”.

Lines 165-187: These two paragraphs should be in the ‘Materials and methods’ section.

Response:

Taking the comment, the two paragraphs is now placed in the 'Materials and methods' section in L185-208.

Line 253: The observations did not show 'a secondary peak in summer', as the authors presented in line 189 'Winter maxima and summer minima were observed'.

Response:

Taking the comment, the observed results are now described more accurately in L213-214 as "Winter maxima were observed for the four sites, while a secondary elevation was observed for Alert and Tiksi."

Descriptions on the simulated results were revised in L284-285 as "This seasonality agrees with observations and simulations at Alert, Tiksi, and Barrow if consider the unintentional data exclusion (Stohl et al., 2013),...".

Line 276-278: What caused the difference between this study (18%) and Winiger et al. (2019) (39%)? Can the different emissions (2010 vs 2011-2015) lead to the doubled contribution?

Response:

We appreciate for the comment. Winiger et al. (2019) included open field burning and residential biofuel burning as the total biomass burning. In the current study, residential burning of biofuels and fossil fuels, and open biomass burning altogether contributed 33% to Arctic surface BC. Such results indicated that the contribution of biomass burning (residential burning of biofuels and open burning) to Arctic surface BC in the current study is smaller than those by Winiger et al. (2019). Such a difference could be attributed the different treatment of BC removal by models (versions 9 and 10), as well as the different emission data.

These discussions were added in L323-332 as "A recent study based on isotope observations at the Arctic sites and Flexpart v9.2 simulation suggested that open biomass burning, including open field burning and residential biofuel burning, contributed 39 % of annual BC in 2011–2015 (Winiger et al., 2019) (Table 1). In comparison, we estimated that residential burning and open biomass burning together account for 33 % of total Arctic surface BC. As the residential burning in our study includes burning of both biofuels and fossil fuels, our results indicated that biomass burning has a relatively smaller contribution. Other than the differences in BC removal treatment between different versions of the model, the contribution difference could also be attributed to the different emission inventories and years (2010 versus 2011-2015)".

Response to comments by reviewer#2

This manuscript presents the source apportionment of black carbon at surface (0-500 m) and high altitudes (4750-5250 m) over the Arctic region using the latest version of Flexpart model. This study provides interesting data specifying the contributions of anthropogenic and biomass burning sources from different source regions to the surface and high altitude Arctic BC that significantly contribute to the Arctic aerosol community. However, discussion needs to be improved further before the MS appears in ACP.

Response:

We appreciate the reviewer for the positive evaluations on our work. Taking the comments, we added new analyses and revised discussions. Each of the comments is responded as follows.

Specific comments: Lines 24-25: “— with a focus on — 2010.” It is not clear in the abstract and in the whole text as well that whether the two source categories (i) anthropogenic activities include only the fossil fuel combustion (or human made such as domestic and agricultural biomass burning as well) and (ii) biomass burning includes only the forest fires (or human made biomass burning as well)!

Response: We apologize for the unclear description of such an important point. In this study, (i) anthropogenic activities include not only fossil fuel combustion, but also human made domestic burning of biofuels; while (ii) the term of biomass burning was intended to denote open biomass burning in the field, includes forest fires, peat fires, open burnings of agricultural waste, grassland and savanna, woodland, deforestation and degradation. For clarity, we changed the term from “biomass burning” to “open biomass burning” throughout the text and added descriptions in the method section.

In the Abstract, the general introduction was revised in L24-26 as, “Geospatial sources of Arctic BC were quantified, with a focus on emissions from anthropogenic activities (including domestic biofuel burning) and open biomass burning (including agricultural burning in the open field) in 2010”.

Descriptions about anthropogenic BC emissions were revised in L160-164 as “The Hemispheric Transport of Air Pollution version 2 inventory (HTAP2) for 2010 was used for monthly anthropogenic BC emissions (Janssens-Maenhout et al., 2015), which include sectors from energy, industry, residential and transport. It is worth noting that the residential sector includes not only combustions of fossil fuels, but also biofuels”.

Descriptions about open biomass burning BC emissions were revised in L170-173 as “The term “open biomass burning” here indicates burning of biomass in the open field as is determined by the remote sensing measurement basis, including forest, agricultural waste, peat fires, grassland and savanna, woodland, deforestation and degradation, where biofuel burning for residential use is not included”.

Lines 58-92: The review of literature of Arctic BC and its sources appears very brief. It is necessary to describe it fully by detailing the previous studies and thus addressing the necessity of the present study.

Response:

Taking the comments, we newly summarized current progress about Arctic BC source estimation in Table 1, where major BC source regions/sectors, model types, settings, meteorology, emission inventories, etc. were included. The description in the context was revised accordingly.

For the simulation of Arctic BC, the treatment of wet-scavenging parameterizations is a key factor affecting the model performance. With the new wet-scavenging scheme, Flexpart v10 cloud water treatment is much improved comparing with its previous versions. We therefore applied Flexpart v10 to investigate Arctic BC source, a first study of its kind as far as we know. We now revised the context to addressing the necessity of the study clearer.

In L79-81, we added “With these large disagreements among studies, it is thus necessary to unveil BC sources in the Arctic with high precision simulations”.

In L87-89, we revised as “... (Table 1). The treatment of wet-scavenging parameterizations is a key factor affecting the model performance, which determines the uncertainties related to BC particle removal (Kipling et al., 2013; Schacht et al., 2019; Q. Wang et al., 2014)”.

In L96-108, we placed as “The FLEXible PARTicle dispersion model (Flexpart) had been used to investigate the transport pathways and source contributions of BC in the Arctic (Stohl et al., 1998, 2006, 2013). Of Flexpart model up to version 9, wet removal was treated considering below-cloud and within-cloud scavenging processes (Hertel et al., 1995; McMahon and Denison, 1979), which depends on cloud liquid water content, precipitation rate and the depth of the cloud. However, clouds were parameterized based on relative humidity, clouds frequently extended to the surface and at times no clouds could be found in grid cells, with unrealistic precipitation (Grythe et al., 2017). Recently, version 10 of Flexpart had been developed in which cloud is differentiated into liquid, solid, and mixed phase, the cloud distribution is more consistent with the precipitation data (Grythe et al., 2017). This improvement in the cloud distribution and phase leads to a more realistic distribution of below-cloud and in-cloud scavenging events. In this study, we quantified region-separated sources of BC in the Arctic in 2010 by using Flexpart v10.1”.

Lines 188~: “Flexpart generally reproduced the seasonal variations —” Lines 200~: Flexpart v10.1 underestimated observed BC —” I suggest the authors to compare the ground based and estimated concentrations, rather than just correlations, which are medium ($r = 0.53-0.80$) only, and statements, in order to make the extent of differences / uncertainties' clear.

Response:

Taking the comments, we added the comparisons of the concentrations, in L220-224 as “From January to May at Barrow and Alert, the mean BC simulated by Flexpart v10.1 were 32.2 ng m^{-3} and 31.2 ng m^{-3} , respectively. Which was 46 % lower than the observations

(59.3 ng m⁻³ and 58.2 ng m⁻³, respectively). This is probably related to the inadequate BC emission in the inventory, although seasonal variations in residential heating are included in HTAP2, which would reduce the simulation bias (Xu et al., 2017)".

In L230-231, we revised as "At Zeppelin, the Flexpart-simulated BC (39.1 ng m⁻³ for annual mean) was 85 % higher than the observed value (21.1 ng m⁻³ for annual mean), especially in winter (112% higher).".

In L236-241, we revised as "At Tiksi, Flexpart underestimated BC (74.4 ng m⁻³ for annual mean) in comparison with observation (104.2 ng m⁻³ for annual mean). Other than the hydrophilic BC assumption and underestimated BC emission in the simulation as the cases for Barrow and Alert, the observations at Tiksi by an aethalometer could contain light-absorbing particles other than BC, resulting in higher observed concentrations if compared with those obtained by SP2, EC and PSAP".

Lines 255~: "This seasonality ---" It is not at all clear that how good the results obtained in the present study are in agreement with the previous reports and how advanced /differed the source assessment of Arctic BC obtained from this study compared to the previous reports. For example, Stohl et al. 2013 reported that gas flaring and domestic biomass burning are the major sources of Arctic BC. This study also showed that the gas flaring is a major source, but the role of domestic biomass burning is not clear.

Response: Taking the comments, we newly evaluated the sectorial contributions to Arctic BC in Figure 5. We found that residential combustions are important sources of Arctic surface BC (36% in October-March), results being similar with those by Stohl et al. (2013). Meanwhile, we estimated a higher value of gas flaring source BC (annually 17.5 ng m⁻³, 36% of total) than those by Stohl et al. (2013). Such a difference could be caused by the model treatment of BC removal as well as the inventory differences.

We added such comparisons in L305-322, as "On an annual basis, anthropogenic sources and open biomass burning emissions accounted for 82 % and 18 %, respectively, of total Arctic surface BC. In which, gas flaring and residential burning (including burning of fossil fuels and biofuels) are accounting for 36 % (28–57 % in October–March) and 15 % (13–25 % in October–March), respectively (Fig. 5a-b). Our results support Stohl et al. (2013) that residential combustion emissions, especially in winter are important sources of Arctic BC (Table 1). We estimated a contribution of gas flaring to Arctic surface BC of 17.5 ng m⁻³ (36% of total). In comparison, the value was estimated as 11.8 ng m⁻³ using an average Arctic surface BC of 28 ng m⁻³ and a fraction from gas flaring of 42 % evaluated by earlier versions of Flexpart (Stohl et al., 2013; Winiger et al., 2019). The different contribution could be partly attributed to the difference in gas flaring emission inventory. BC emission from gas flaring in Russia by Huang et al. (2015) was used in the current study, where total BC emission from gas flaring in Russia in 2010 was ca. 81.1 kilotonne, which was larger than the estimate of ca. 64.9 kilotonne by GAINS inventory (Klimont et al., 2017) used by Stohl et al. (2013). Moreover, Adopting ECLIPSEv5 inventory as was used by Winiger et al. (2019), we estimated that gas flaring was contributing 14.4 ng m⁻³ to Arctic surface BC using Flexpart v10.1, a value 22 % higher than those obtained using Flexpart v9. This difference could be attributed to the improvement of the wet-scavenging scheme by Flexpart v10.1".

Newly added Figure 5:

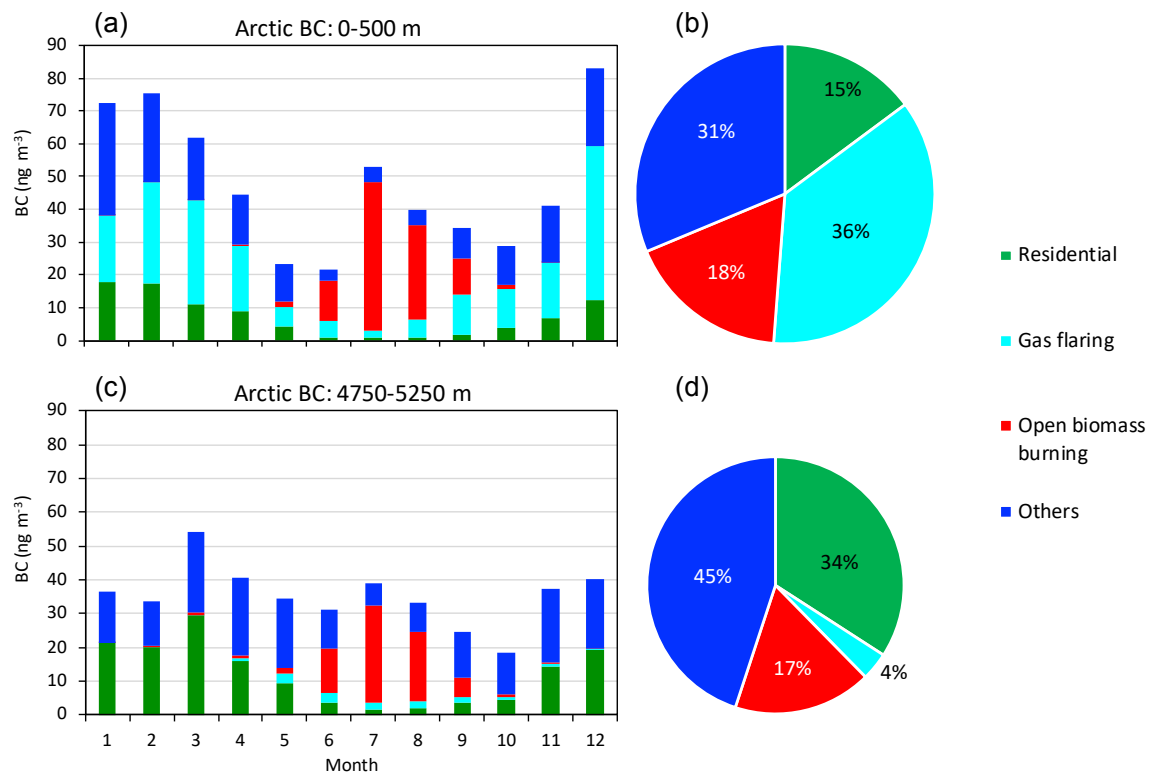


Figure 5. Sectorial contributions from residential combustion (including fossil fuel and biofuel combustions), gas flaring, open biomass burning and others (energy other than gas flaring, industry and transport) to (a) seasonal variations in Arctic surface BC, (b) annual mean Arctic surface BC, (c) seasonal variations in Arctic BC at high altitudes, and (d) annual mean of Arctic BC at high altitudes.

1 **Flexpart v10.1 simulation of source contributions to Arctic black carbon**

2

3 Chunmao Zhu¹, Yugo Kanaya^{1,2}, Masayuki Takigawa^{1,2}, Kohei Ikeda³, Hiroshi Tanimoto³,

4 Fumikazu Taketani^{1,2}, Takuma Miyakawa^{1,2}, Hideki Kobayashi^{1,2}, Ignacio Pissó⁴

5

6 ¹Research Institute for Global Change, Japan Agency for Marine–Earth Science and
7 Technology (JAMSTEC), Yokohama 2360001, Japan

8 ²Institute of Arctic Climate and Environmental Research, Japan Agency for Marine–Earth
9 Science and Technology, Yokohama 2360001, Japan

10 ³National Institute for Environmental Studies, Tsukuba 305-8506, Japan

11 ⁴NILU – Norwegian Institute for Air Research, Kjeller 2027, Norway

12

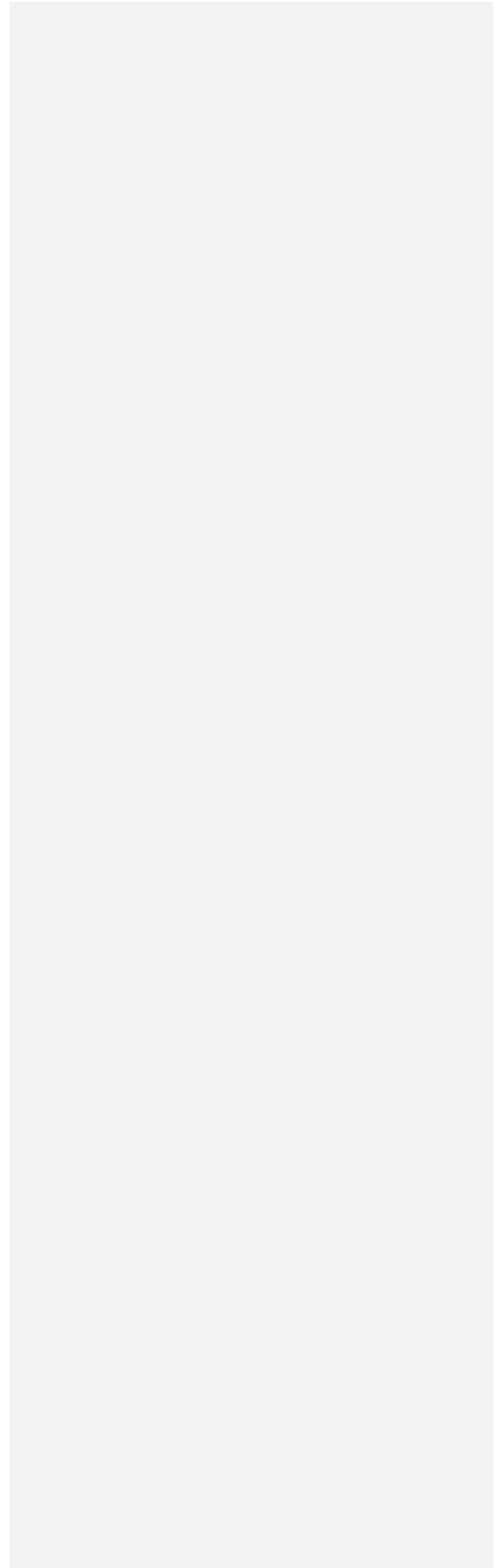
13 Correspondence to Chunmao Zhu (chmzhu@jamstec.go.jp)

14 Abstract

15 The Arctic environment is undergoing rapid changes such as faster warming than the
16 global average and exceptional melting of glaciers in Greenland. Black carbon (BC) particles,
17 which are a short-lived climate pollutant, are one cause of Arctic warming and glacier
18 melting. However, the sources of BC particles are still uncertain. We simulated the potential
19 emission sensitivity of atmospheric BC present over the Arctic (north of 66° N) using the
20 Flexpart Lagrangian transport model (version 10.1). This version includes a new aerosol wet
21 removal scheme, which better represents particle-scavenging processes than older versions
22 did. Arctic BC at the surface (0–500 m) and high altitudes (4750–5250 m) is sensitive to
23 emissions in high latitude (north of 60° N) and mid-latitude (30–60° N) regions, respectively.
24 Geospatial sources of Arctic BC were quantified, with a focus on emissions from
25 anthropogenic activities [\(including domestic biofuel burning\)](#) and [open](#) biomass burning
26 [\(including agricultural burning in the open field\)](#) in 2010. We found that anthropogenic
27 sources contributed 82 % and 83 % of annual Arctic BC at the surface and high altitudes,
28 respectively. Arctic surface BC comes predominantly from anthropogenic emissions in
29 Russia (56 %), with gas flaring from the Yamalo-Nenets Autonomous Okrug and Komi
30 Republic being the main source (31 % of Arctic surface BC). These results highlight the need
31 for regulations to control BC emissions from gas flaring to mitigate the rapid changes in the
32 Arctic environment. In summer, combined [open](#) biomass burning in Siberia, Alaska, and
33 Canada contributes 56–85 % (75 % on average) and 40–72 % (57 %) of Arctic BC at the
34 surface and high altitudes, respectively. A large fraction (40 %) of BC in the Arctic at high
35 altitudes comes from anthropogenic emissions in East Asia, which suggests that the rapidly
36 growing economies of developing countries could have a non-negligible effect on the Arctic.
37 To our knowledge, this is the first year-round evaluation of Arctic BC sources that has been

Deleted:

39 performed using the new wet deposition scheme in Flexpart. The study provides a scientific
40 basis for actions to mitigate the rapidly changing Arctic environment.
41



42 **1 Introduction**

43 The Arctic region has experienced warming at a rate twice that of the global average in
44 recent decades (Cohen et al., 2014). The Arctic cryosphere has been undergoing
45 unprecedented changes since the mid-1800s (Trusel et al., 2018). Glacier cover in Greenland
46 reached its historically lowest level in summer 2012 (Tilling et al., 2015). Evidence indicates
47 that the emissions and transport of greenhouse gases and aerosols to the Arctic region are
48 contributing to such warming and melting of snow and ice (Keegan et al., 2014; Najafi et al.,
49 2015). Short-lived climate pollutants such as black carbon (BC) particles, tropospheric ozone,
50 and methane greatly affect the Arctic climate (AMAP, 2015; Quinn et al., 2008).

51 BC particles are emitted during incomplete combustion of fossil fuels, biofuels, and
52 biomass. BC warms the atmosphere by direct absorption of solar radiation. The deposition
53 of BC on snow and ice surfaces accelerates their melting through decreasing albedo, which
54 contributes to the rapid loss of glaciers. In the Arctic region, ground-based observations
55 have indicated that BC shows clear seasonal variations, with elevated mass concentrations
56 in winter and spring (the so-called Arctic haze) and low values in summer (Law and Stohl,
57 2007). Such seasonal variations are explained by increased transport from lower latitudes in
58 the cold season and increased wet scavenging in the warm season (Shaw, 1995; Garrett et
59 al., 2011; Shen et al., 2017).

60 The presence of BC particles in the Arctic is mainly attributed to emissions in high-latitude
61 regions outside the Arctic, such as northern Europe and Russia (Stohl, 2006; Brock et al.,
62 2011). This is partly caused by the polar dome (Stohl, 2006), which is formed because of the
63 presence of constant potential temperature near the surface. The emissions in high-latitude
64 regions are transported to the Arctic region and trapped in the dome, which increases the
65 surface concentration. Recently, Schmale et al. (2018) suggested that local emissions from

66 within the Arctic are another important source, and these are expected to increase in the
67 future.

68 Although numerous studies have been performed, results regarding regional
69 contributions of BC sources in the Arctic are still inconclusive. For example, ground-based
70 observations and Lagrangian transport model results reported by Winiger et al. (2016)
71 showed that BC in Arctic Scandinavia is predominantly linked to emissions in Europe. Over
72 the whole Arctic region (north of 66° N), Russia contributes 62 % to surface BC in terms of
73 the annual mean (Ikeda et al., 2017). Gas flaring in Russia has been identified as a major
74 (42 %) source of BC at the Arctic surface (Stohl et al., 2013). Xu et al. (2017) found that
75 anthropogenic emissions from northern Asia contribute 40–45 % of Arctic surface BC in
76 winter and spring. However, the results of some other studies have suggested that Russia,
77 Europe, and South Asia each contribute 20–25 % of BC to the low-altitude springtime Arctic
78 haze (Koch and Hansen, 2005). Sand et al. (2016) found that the surface temperature in the
79 Arctic is most sensitive to emissions in Arctic countries, and Asian countries contribute
80 greatly to Arctic warming because of the large absolute amount of emissions. With these
81 large disagreements among studies, it is thus necessary to unveil BC sources in the Arctic
82 with high precision simulations.

83 Various models have been used to investigate BC sources in the Arctic. Depending on the
84 simulation method, these models are generally categorized as Lagrangian transport models
85 (Hirdman et al., 2010; Liu et al., 2015; Stohl et al., 2006, 2013), chemical transport models
86 (Ikeda et al., 2017; Koch and Hansen, 2005; Qi et al., 2017; Shindell et al., 2008; Wang et al.,
87 2011; Xu et al., 2017), and global climate models (Ma et al., 2013; Schacht et al., 2019; H.
88 Wang et al., 2014) (Table 1). The treatment of wet-scavenging parameterizations is a key
89 factor affecting the model performance, which determines the uncertainties related to BC

Deleted: The

Deleted: of the simulations are mainly generated from the
model treatment of processes for

93 particle removal (Kipling et al., 2013; Schacht et al., 2019; Q. Wang et al., 2014). The use of
 94 emission inventories is another important factor that affects the simulation results (Dong et
 95 al., 2019). The observations of BC that are used for model comparisons may be biased by
 96 30 % depending on the method used (Sinha et al., 2017; Sharma et al., 2017). There are still
 97 large uncertainties regarding the sources of BC in the Arctic with respect to emission sectors
 98 (anthropogenic sources and open biomass burning) and geospatial contributions (Eckhardt
 99 et al., 2015).

100 The FLEXible PARTicle dispersion model (Flexpart) had been used to investigate the
 101 transport pathways and source contributions of BC in the Arctic (Stohl et al., 1998, 2006,
 102 2013). Of Flexpart model up to version 9, wet removal was treated considering below-cloud
 103 and within-cloud scavenging processes (Hertel et al., 1995; McMahon and Denison, 1979),
 104 which depends on cloud liquid water content, precipitation rate and the depth of the cloud.
 105 However, clouds were parameterized based on relative humidity, clouds frequently
 106 extended to the surface and at times no clouds could be found in grid cells, with unrealistic
 107 precipitation (Grythe et al., 2017). Recently, version 10 of Flexpart had been developed in
 108 which cloud is differentiated into liquid, solid, and mixed phase, the cloud distribution is
 109 more consistent with the precipitation data (Grythe et al., 2017). This improvement in the
 110 cloud distribution and phase leads to a more realistic distribution of below-cloud and in-
 111 cloud scavenging events. In this study, we quantified region-separated sources of BC in the
 112 Arctic in 2010 by using Flexpart v10.1. We first evaluated the model performance by
 113 comparing the results with those based on observations at surface sites. The source
 114 contributions of emission sectors and geospatial contributions were evaluated by
 115 incorporating the Arctic BC footprint into the emission inventories.

116 2 Materials and methods

Deleted: , especially wet-scavenging processes

Moved (insertion) [3]

Deleted: In the older

Deleted: s

Deleted: o

Deleted: f Flexpart

Deleted: in which

Deleted: In comparison,

Deleted: in

Deleted: v10.1,

Deleted: version

Deleted: of the FLEXible PARTicle dispersion model
(Flexpart) (Stohl et al., 1998, 2006, 2013; Grythe et al., 2017)

129 2.1 Transport model

130 The Flexpart model (version 10.1) was run in backward mode to simulate BC footprints in
131 the Arctic region. The calculation of wet deposition was improved compared with those in
132 previous versions because in-cloud scavenging and below-cloud scavenging of particles were
133 separately calculated (Grythe et al., 2017). In previous versions of Flexpart, in the in-cloud
134 scavenging scheme, the aerosol scavenging coefficient depended on the cloud water
135 content, which was calculated according to an empirical relationship with precipitation rate,
136 in which all aerosols had the same nucleation efficiency (Hertel et al., 1995 ; Stohl et al.,
137 2005). In the new version, the in-cloud scavenging scheme depends on the cloud water
138 phase (liquid, ice, or mixed phase). Aerosols were set as ice nuclei for ice clouds and as
139 cloud condensation nuclei for liquid-water clouds, respectively. For mixed-phase clouds, it
140 was assumed that 10 % of aerosols are ice nuclei and 90 % are cloud condensation nuclei,
141 because BC is much more efficiently removed in liquid water clouds than in ice clouds (Cozic
142 et al., 2007; Grythe et al., 2017). The below-cloud scavenging scheme can parameterize
143 below-cloud removal as a function of aerosol particle size, and precipitation type (snow or
144 rain) and intensity. The biases produced in simulations using the new scheme are therefore
145 smaller than those in the old scheme for wet deposition of aerosols, especially at high
146 latitudes (Grythe et al., 2017).

147 The Arctic region is defined as areas north of 66° N. The potential BC emission
148 sensitivities at two heights in the Arctic region, i.e., the surface (0–500 m) and 5000 m
149 (4750–5250 m), were simulated. The Flexpart outputs were set as gridded retention times.
150 We performed tests at 500, 2000, and 5000 m, and chose 500 m as the upper boundary
151 height of the model output. The model was driven with operational analytical data from the
152 European Centre for Medium-Range Weather Forecasts (ECMWF) at a spatial resolution of

153 $1^\circ \times 1^\circ$ with 61 vertical levels. Temporally, ECMWF has a resolution of 3 h, with 6 h analysis
154 and 3 h forecast time steps. The simulation period was set at 60 days backward starting
155 from each month in 2010. The maximum life time of BC was set at 20 days because its
156 suspension time in the upper atmosphere during long-range transport is longer than that at
157 the surface level (Stohl et al., 2013). We implemented the wet deposition scheme in the
158 backward calculations, but it was not represented in the default setting (Flexpart v10.1,
159 <https://www.flexpart.eu/downloads>, obtained 10 April 2017).

160 The chemistry and microphysics could not be resolved by Flexpart. The model therefore
161 ignores hydrophobic to hydrophilic state changes and size changes of BC, and assumes that
162 all BC particles are aged hydrophilic particles. This may lead to an overestimation of BC
163 removal and hence force underestimation of simulated BC concentration, especially of fossil
164 fuel combustion sources where BC could be in the hydrophobic state for a few days. A
165 logarithmic size distribution of BC with a mean diameter of $0.16 \mu\text{m}$ and a standard
166 deviation of 1.96, in accordance with our ship observations in the Arctic, was used (Taketani
167 et al., 2016). The particle density was assumed to be 2000 kg m^{-3} , and 1 million
168 computational particles were randomly generated in the Arctic region for the backward
169 runs.

170 Four ground-based observations made during the period 2007–2011 were used to
171 validate the model performance. The potential BC emission sensitivity at 0–500 m above
172 ground level from a 0.1° grid centered at each site was simulated. Other model
173 parameterizations were consistent with those for the Arctic region, except that 200 000
174 computational particles were released.

175 2.2 Emission inventories

176 We focused on BC sources from anthropogenic emissions and open biomass burning. The
177 Hemispheric Transport of Air Pollution version 2 inventory (HTAP2) for 2010 was used for
178 monthly anthropogenic BC emissions (Janssens-Maenhout et al., 2015), which include
179 sectors from energy, industry, residential and transport. It is worth noting that the
180 residential sector includes not only combustions of fossil fuels, but also biofuels. However,
181 as it has been reported that BC emissions in Russia were underestimated in HTAP2, we used
182 the BC emissions reported by Huang et al. (2015) for Russia, in which the annual BC
183 emissions were 224 Gg yr⁻¹. For open biomass burning, we used the monthly BC emissions
184 from the Global Fire Emissions Database version 3 inventory (GFED3) (van der Werf et al.,
185 2010) for the purposes of intercomparison with other studies, as this version is widely used.
186 The term “open biomass burning” here indicates burning of biomass in the open field as is
187 determined by the remote sensing measurement basis, including forest, agricultural waste,
188 peat fires, grassland and savanna, woodland, deforestation and degradation, where biofuel
189 burning for residential use is not included. Geospatial distributions of emissions from
190 anthropogenic sources and open biomass burning in January and July are shown in Fig. S1.

191 2.3 Calculation of Arctic BC source contributions

192 The source contributions to Arctic BC were derived by incorporating the gridded
193 retention time into the column emission flux, which was derived from the emission
194 inventories in each grid. Calculations for anthropogenic sources and open biomass burning
195 were performed separately and the sum was used. For anthropogenic sources, the regions
196 were separated into North America and Canada (25–80° N, 50–170° W), Europe (30–80° N,
197 0–30° E), Russia (53–80° N, 30–180° E), East Asia (35–53° N, 75–150° E and 20–35° N, 100–
198 150° E), and others (the rest) (Fig. 1a). For open biomass burning sources, the regions were

Deleted: .

Deleted: -

201 separated into Alaska and Canada (50–75° N, 50–170° W), Siberia (50–75° N, 60–180° E),
202 and others (Fig. 1b).

203 2.3 Observations

204 BC levels simulated by Flexpart were compared with those based on surface observations
205 at four sites: Barrow, USA (156.6° W, 71.3° N, 11 m asl), Alert, Canada (62.3° W, 82.5° N,
206 210 m asl), Zeppelin, Norway (11.9° E, 78.9° N, 478 m asl), and Tiksi, Russia (128.9° E, 71.6°
207 N, 8 m asl). Aerosol light absorption was determined by using particle soot absorption
208 photometers (PSAPs) at Barrow, Alert, and Zeppelin, and an aethalometer at Tiksi. For PSAP
209 measurements, the equivalent BC values were derived using a mass absorption efficiency of
210 10 m² g⁻¹. The equivalent BC at Tiksi, which was determined with an aethalometer, was
211 obtained directly. These measurement data were obtained from the European Monitoring
212 and Evaluation Programme and World Data Centre for Aerosols database
213 (<http://ebas.nilu.no>) (Tørseth et al., 2012).

214 It is worth noting that uncertainties could be introduced by using different BC
215 measurement techniques. An evaluation of three methods for measuring BC at Alert,
216 Canada indicated that an average of the refractory BC determined with a single-particle soot
217 photometer (SP2) and elemental carbon (EC) determined from filter samples give the best
218 estimate of BC mass (Sharma et al., 2017). Xu et al. (2017) reported that the equivalent BC
219 determined with a PSAP was close to the average of the values for refractory BC and EC at
220 Alert. In this study, we consider that the equivalent BC values determined with a PSAP at
221 Barrow, Alert, and Zeppelin to be the best estimate. There may be uncertainties in the
222 equivalent BC observations performed with an aethalometer at Tiksi because of co-existing
223 particles such as light-absorptive organic aerosols, scattering particles, and dusts
224 (Kirchstetter et al., 2004; Lack and Langridge, 2013). Interference by the filter and

Formatted: Indent: First line: 0 cm

Moved (insertion) [1]

225 uncertainties in the mass absorption cross section could also contribute to the bias
 226 observed in measurements made with an aethalometer at Tiksi.

227 3 Results and discussion

228 3.1. Comparisons of simulations with BC observations at Arctic surface sites

229 Flexpart generally reproduced the seasonal variations in BC at four Arctic sites well
 230 [Pearson correlation coefficient (R) = 0.53–0.80, root-mean-square error (RMSE) = 15.1–56.8
 231 ng m⁻³] (Fig. 2). Winter maxima were observed for the four sites, while a secondary
 232 elevation was observed for Alert and Tiksi. At Barrow, the observed high values of BC were
 233 unintentionally excluded during data screening in the forest fire season in summer (Stohl et
 234 al., 2013); the original observed BC is supposed to be higher as was reflected by the
 235 simulation. This seasonality is probably related to relatively stronger transport to the Arctic
 236 region in winter, accompanied by lower BC aging and inefficient removal, as simulated by
 237 older versions of Flexpart (Eckhardt et al., 2015; Stohl et al., 2013).

238 From January to May at Barrow and Alert, the mean BC simulated by Flexpart v10.1 were
 239 32.2 ng m⁻³ and 31.2 ng m⁻³, respectively. Which was 46 % lower than the observations
 240 (59.3 ng m⁻³ and 58.2 ng m⁻³, respectively). This is probably related to the inadequate BC
 241 emission in the inventory, although seasonal variations in residential heating are included in
 242 HTAP2, which would reduce the simulation bias (Xu et al., 2017). Simulations by GEOS-Chem
 243 using the same emission inventories also underestimated BC levels at Barrow and Alert
 244 (Ikeda et al., 2017; Xu et al., 2017). The underestimation by Flexpart could also be partly
 245 contributed by the assumption that all particles are hydrophilic, where the BC scavenging
 246 could be overestimated. The corresponding uncertainties are larger in winter months, when
 247 there are more sources from fossil fuel combustion.

Moved up [1]: BC levels simulated by Flexpart were compared with those based on surface observations at four sites: Barrow, USA (156.6° W, 71.3° N, 11 m asl), Alert, Canada (62.3° W, 82.5° N, 210 m asl), Zeppelin, Norway (11.9° E, 78.9° N, 478 m asl), and Tiksi, Russia (128.9° E, 71.6° N, 8 m asl). Aerosol light absorption was determined by using particle soot absorption photometers (PSAPs) at Barrow, Alert, and Zeppelin, and an aethalometer at Tiksi. For PSAP measurements, the equivalent BC values were derived using a mass absorption efficiency of 10 m² g⁻¹. The equivalent BC at Tiksi, which was determined with an aethalometer, was obtained directly. These measurement

Deleted: . ¶ ... [1]

Deleted: and summer minima

Deleted: [Pearson correlation coefficient (R) = 0.53–0.80, root-mean-square error (RMSE) = 15.1–56.8 ng m⁻³]. It was ... [2]

Moved (insertion) [2]

Deleted: by local pollution

Deleted: from the data set for Barrow

Deleted: the notably

Deleted: level

Deleted: of

Deleted: ed BC may reflect this.

Deleted:

Moved up [3]: In the older versions of Flexpart, in which clouds were parameterized based on relative humidity,

Deleted: underestimated observed BC in January to May at Barrow and Alert, and in most months at Tiksi.

Deleted: used

347 At Zeppelin, the Flexpart-simulated BC (39.1 ng m⁻³ for annual mean) was 85 % higher
 348 than the observed value (21.1 ng m⁻³ for annual mean), especially in winter (112% higher). It
 349 has been reported that riming in mixed-phase clouds occurs frequently at Zeppelin (Qi et al.,
 350 2017). During the riming process, BC particles act as ice particles and collide with the
 351 relatively numerous water drops, which form frozen cloud droplets, and then snow is
 352 precipitated. This results in relatively efficient BC scavenging (Hegg et al., 2011). Such a
 353 process could not be dealt with by the model. At Tiksi, Flexpart underestimated BC (74.4 ng
 354 m⁻³ for annual mean) in comparison with observation (104.2 ng m⁻³ for annual mean). Other
 355 than the hydrophilic BC assumption and underestimated BC emission in the simulation as
 356 the cases for Barrow and Alert, the observations at Tiksi by an aethalometer could
 357 containing light-absorbing particles other than BC, resulting in higher observed
 358 concentrations if compared with those obtained by SP2, EC and PSAP.

359 Anthropogenic emissions are the main sources of BC at the four Arctic sites from late
 360 autumn to spring, whereas open biomass burning emissions make large contributions in
 361 summer. From October to April, anthropogenic emissions accounted for 87–100 % of BC
 362 sources at all the observation sites. At Barrow, open biomass burning accounted for 35–
 363 78 % of BC in June–September (Fig. 2). There are large interannual variations in both
 364 observed and simulated BC (Fig. S2). In June–August 2010, the mean contributions of open
 365 biomass burning to BC were 6.3, 2.4, and 8.6 times those from anthropogenic sources at
 366 Alert, Zeppelin, and Tiksi, respectively. In this study, we focused on BC in the Arctic region in
 367 2010.

368 3.2 Potential emission sensitivity of Arctic BC

369 The potential emission sensitivities (footprint) of Arctic BC showed different patterns
 370 with respect to altitude. The Arctic surface is sensitive to emissions at high latitudes (>60°

Deleted: -

Deleted: 54

Deleted: a

Moved up [2]: It was reported that observed high values of BC were unintentionally excluded by local pollution data screening from the data set for Barrow in the forest fire season in summer (Stohl et al., 2013); the notably higher level of simulated BC may reflect this.

Deleted: 86

Deleted: ~9.8,

Deleted: Barrow,

382 N). Air masses stayed for over 60 s in each of the 1° grids from the eastern part of northern
383 Eurasia and the Arctic Ocean before being transported to the Arctic surface in the winter,
384 represented by January (Fig. 3a). In comparison, during the summer, represented by July, BC
385 at the Arctic surface was mainly affected by air masses that originated from the Arctic
386 Ocean and the Norwegian Sea (Fig. 3b). These results imply that local BC emissions within
387 the Arctic regions, although relatively weak compared with those from the mid-latitude
388 regions, could strongly affect Arctic air pollution. Local BC emissions are important in the
389 wintertime because the relatively stable boundary layer does not favor pollution dispersion.
390 Recent increases in anthropogenic emissions in the Arctic region, which have been caused
391 by the petroleum industry and development of the Northern Sea Route, are expected to
392 cause deterioration of air quality in the Arctic. Socio-economic developments in the Arctic
393 region would increase local BC emissions, and this will be a non-negligible issue in the future
394 (Roiger et al., 2015; Schmale et al., 2018).

395 BC at high altitudes (~ 5000 m) in the Arctic is more sensitive to mid-latitude (30–60° N)
396 emissions, especially in wintertime. In January, air masses hovered over the Bering Sea and
397 the North Atlantic Ocean before arriving at the Arctic (Fig. 3c). A notable corridor at 30–50°
398 N covering Eurasia and the United States was the sensitive region that affected BC at high
399 altitudes in the Arctic in January. These results indicate that mid-latitude emissions,
400 especially those with relatively large strengths from East Asia, East America, and Europe,
401 could alter the atmospheric constituents at high altitudes in the Arctic. Central to east
402 Siberia was the most sensitive region for BC at high altitudes in the Arctic in July (Fig. 3d).
403 These results suggest that pollutants from frequent and extensive wildfires in Siberia in
404 summer are readily transported to high altitudes in the Arctic. Boreal fires are expected to
405 occur more frequently and over larger burning areas under future warming (Veira et al.,

406 2016), therefore the atmospheric constituents and climate in the Arctic could undergo more
407 rapid changes.

408 3.3 Seasonal variations and sources of Arctic surface BC

409 Arctic surface BC showed clear seasonal variations, with a primary peak in winter–spring
410 (December–March, 61.8–82.8 ng m⁻³) and a secondary peak in summer (July, 52.7 ng m⁻³).

411 BC levels were relatively low in May–June (21.8–23.1 ng m⁻³) and September–November
412 (34.1–40.9 ng m⁻³) (Fig. 4a). This seasonality agrees with observations and simulations at
413 Alert, Tiksi, and Barrow if consider the unintentional data exclusion (Stohl et al., 2013), and
414 previous studies targeting the whole Arctic (Ikeda et al., 2017; Xu et al., 2017). Compared
415 with the study reported by Stohl et al. (2013), the current work using the new scheme
416 produced smaller discrepancies between the simulated data and observations. Although the
417 simulation periods (monthly means for 2007–2011 in this study and for 2008–2010 in the
418 old scheme) and the anthropogenic emission inventories (HTAP2 in this study and ECLIPSE4
419 in the previous study) are different, the new scheme shows potential for better representing
420 BC transport and removal processes in the Arctic.

421 The annual mean Arctic BC at the surface was estimated to be 48.2 ng m⁻³. From October
422 to April, anthropogenic sources accounted for 96–100 % of total BC at the Arctic surface.
423 Specifically, anthropogenic emissions from Russia accounted for 61–76 % of total BC in
424 October–May (56 % annually), and was the dominant sources of Arctic BC at the surface.
425 From an isentropic perspective, the meteorological conditions in winter favored the
426 transport of pollutants from northern Eurasia to the lower Arctic, along with diabatic cooling
427 and strong inversions (Klonecki et al., 2003). In comparison, open biomass burning from
428 boreal regions accounted for 56–85 % (75 % on average) of Arctic BC at the surface in
429 summer; open biomass burning emissions from North America and Canada accounted for

Deleted: is in agreement

Deleted: Arctic sites (Barrow,

Deleted: and

Deleted:)

Deleted: -

435 54 % of total Arctic surface BC in June, and those from Siberia accounted for 59–61 % in
 436 July–August. Wildfires in the boreal forests in summer had a major effect on air quality in
 437 the Arctic.

438 On an annual basis, anthropogenic sources and open biomass burning emissions
 439 accounted for 82 % and 18 %, respectively, of total Arctic surface BC. In which, gas flaring
 440 and residential burning (including burning of fossil fuels and biofuels) are accounting for
 441 36 % (28–57 % in October–March) and 15 % (13–25 % in October–March), respectively (Fig.
 442 5a-b). Our results support Stohl et al. (2013) that residential combustion emissions,
 443 especially in winter are important sources of Arctic BC (Table 1). We estimated a
 444 contribution of gas flaring to Arctic surface BC of 17.5 ng m⁻³ (36% of total). In comparison,
 445 the value was estimated as 11.8 ng m⁻³ using an average Arctic surface BC of 28 ng m⁻³ and
 446 a fraction from gas flaring of 42 % evaluated by earlier versions of Flexpart (Stohl et al.,
 447 2013; Winiger et al., 2019). The different contribution could be partly attributed to the
 448 difference in gas flaring emission inventory. BC emission from gas flaring in Russia by Huang
 449 et al. (2015) was used in the current study, where total BC emission from gas flaring in
 450 Russia in 2010 was ca. 81.1 kilotonne, which was larger than the estimate of ca. 64.9
 451 kilotonne by GAINS inventory (Klimont et al., 2017) used by Stohl et al. (2013). Moreover,
 452 Adopting ECLIPSEv5 inventory as was used by Winiger et al. (2019), we estimated that gas
 453 flaring was contributing 14.4 ng m⁻³ to Arctic surface BC using Flexpart v10.1, a value 22 %
 454 higher than those obtained using Flexpart v9. This difference could be attributed to the
 455 improvement of the wet-scavenging scheme by Flexpart v10.1.

456 A recent study based on isotope observations at the Arctic sites and Flexpart v9.2
 457 simulation suggested that open biomass burning, including open field burning and
 458 residential biofuel burning, contributed 39 % of annual BC in 2011–2015 (Winiger et al.,

Deleted: -

Deleted: In comparison, a

Formatted: Not Superscript/ Subscript

Formatted: Superscript

Deleted: a

Deleted: model

463 2019) (Table 1). In comparison, we estimated that residential burning and open biomass
464 burning together account for 33 % of total Arctic surface BC. As the residential burning in
465 our study includes burning of both biofuels and fossil fuels, our results indicated that
466 biomass burning has a relatively smaller contribution. Other than the differences in BC
467 removal treatment between different versions of the model, the contribution difference
468 could also be attributed to the different emission inventories and years (2010 versus 2011-
469 2015).

470 The geospatial contributions of anthropogenic sources and open biomass burning
471 emissions can be further illustrated by taking January and July as examples. In January, high
472 levels of anthropogenic emissions from Russia (contributing 64 % of Arctic surface BC),
473 Europe (18 %), and East Asia (9 %) were identified (Fig. 6a). Specifically, Yamalo-Nenets
474 Autonomous Okrug in Russia, which has the largest reserves of Russia's natural gas and oil
475 (Filimonova et al., 2018), was the most notable emission hotspot, which suggests gas-flaring
476 sources. The Komi Republic in Russia was also identified as a strong anthropogenic emitter
477 contributing to Arctic surface BC. These gas-flaring industrial regions in Russia (58–69° N,
478 68–81°E) together contributed 33 % and 31 % of Arctic surface BC for January and the
479 annual mean, respectively. Recently, Dong et al. (2019) evaluated BC emission inventories
480 using GEOS-Chem and proposed that using the inventory compiled by Huang et al. (2015)
481 for Russia, in which gas flaring accounted for 36 % of anthropogenic emissions, had no
482 prominent impact on the simulation performance in Russia and the Arctic. They suggested
483 that use of a new global inventory for BC emissions from natural gas flaring would improve
484 the model performance (Huang and Fu, 2016). These results suggest that inclusion of BC
485 emissions from gas flaring on the global scale is necessary for further BC simulations.

Deleted: -

Deleted: 5a

488 In Europe, a relatively high contribution of anthropogenic emissions to Arctic surface BC
 489 in January was made by Poland (50–55° N, 15–24° E, contributing 4 % of Arctic surface BC)
 490 because of relatively large emission fluxes in the region (Fig. S1a). Anthropogenic emissions
 491 from East China, especially those north of ~33° N (33–43° N, 109–126° E), contributed
 492 perceptibly (5 %) to Arctic surface BC.

493 In July, contributions from anthropogenic sources shrank to those from Yamalo-Nenets
 494 Autonomous Okrug and Komi Republic in Russia, and contributed a lower fraction (3 % of
 495 Arctic surface BC) (Fig. 6b). Few open biomass burning sources contributed in January (Fig.
 496 6c), but contributions from open biomass burning to Arctic surface BC in July can be clearly
 497 seen, mainly from the far east of Russia, Canada, and Alaska (Fig. 6d). Open biomass burning
 498 emissions from Kazakhstan, southwest Russia, southern Siberia, and northeast China also
 499 contributed to Arctic surface BC, although at relatively low strengths (Fig. 5d and Fig. S1d).
 500 However, the contributions from open biomass burning could be higher, as the MODIS
 501 burned area, the basis of GFED emission inventories, was underestimated for northern
 502 Eurasia by 16 % (Zhu et al., 2017). Evangeliou et al. (2016) estimated a relatively high
 503 transport efficiency of BC from open biomass burning emissions to the Arctic, which led to a
 504 high contribution, i.e., 60 %, from such sources to BC deposition in the Arctic in 2010. A
 505 recent study suggested that open fires burned in western Greenland in summer (31 July to
 506 21 August 2017) could potentially alter the Arctic air composition and foster glacier melting
 507 (Evangeliou et al., 2019). Although the footprint of Arctic surface BC showed a relatively
 508 weak sensitivity to areas such as forests and tundra, in the boreal regions, pollutants from
 509 boreal wildfires could have greater effects on the Arctic air composition in summer under
 510 future warming scenarios (Veira et al., 2016).

511 3.4 Sources of Arctic BC at high altitudes

Deleted: 5b

Deleted: -

Deleted: 5c

Deleted: 5d

Deleted: Biomass

Deleted: -

518 Arctic BC levels at high altitudes (4750–4250 m) showed the highest levels in spring
 519 (March–April, 40.5–53.9 ng m⁻³), followed by those in late autumn to early winter
 520 (November–January, 36.5–40.0 ng m⁻³), and summer (July–August, 33.0–39.0 ng m⁻³) (Fig.
 521 4c). The annual mean Arctic BC at high altitudes was estimated to be 35.2 ng m⁻³, which is
 522 ca. 73 % of those at the surface. Such a vertical profile is in accordance with those based on
 523 aircraft measurements over the High Canadian Arctic (Schulz et al., 2019). Similarly to the
 524 case for the surface, anthropogenic sources dominated by residential sectors, transport,
 525 industry and energy (excluding gas flaring), accounted for 94–100 % of Arctic BC at high
 526 altitudes in October–May (Figs. 4c, 5c). East Asia accounted for 34–65 % of the total BC in
 527 October–May (40 % annually). In comparison, using the Community Atmosphere Model
 528 version 5 driven by the NASA Modern Era Retrospective-Analysis for Research and
 529 Applications reanalysis data and the IPCC AR5 year 2000 BC emission inventory, H. Wang et
 530 al. (2014) found that East Asia accounted for 23% of BC burden in the Arctic for 1995–2005.
 531 In summer, open biomass burning in the boreal regions accounted for 40–72 % (57 % on
 532 average) of Arctic BC at high altitudes, similar to the source contributions to Arctic surface
 533 BC. Specifically, open biomass burning sources from Siberia accounted for 40–42 % of Arctic
 534 BC at high altitudes in July–August. Annually, anthropogenic sources and open biomass
 535 burning accounted for 83 % (in which residential sources accounted for 34%) and 17 %,
 536 respectively, of total Arctic BC at high altitudes (Figs. 4d, 5d).

537 Further investigations of geospatial contributions to Arctic BC at high altitudes in January
 538 and July provided more details regarding BC sources. In January, the main anthropogenic BC
 539 source in East Asia covered a wide range in China (Fig. 7a). Not only east and northeast
 540 China, but also southwest China (Sichuan and Guizhou provinces) were the major
 541 anthropogenic sources of Arctic BC at high altitudes. In July, anthropogenic sources made a

Deleted:

Deleted: biomass

Deleted: -

Deleted: biomass

Deleted: 5a

547 relatively weak contribution to Arctic BC at high altitudes. The regions that were sources of
548 open biomass burning contributions to Arctic BC at high altitudes were mainly the far east of
549 Siberia, Kazakhstan, central Canada, and Alaska, i.e., similar to the sources of Arctic surface
550 BC. Unlike Arctic surface BC, for which the dominant source regions are at high latitudes in
551 both winter and summer, Arctic BC at high altitudes mainly originates from mid-latitude
552 regions (Figs. 6 and 7). In terms of transport pathways, air masses could be uplifted at low-
553 to-mid latitudes and transported to the Arctic (Stohl, 2006). Further investigations are
554 needed to obtain more details of the transport processes.

555 3.5 Comparison of Flexpart and GEOS-Chem simulations of BC sources

556 Data for BC sources simulated with Flexpart were compared with those obtained with
557 GEOS-Chem (Ikeda et al., 2017), which is an Eulerian atmospheric transport model, using the
558 same emission inventories. The simulated seasonal variations in Arctic BC levels and source
559 contributions obtained with Flexpart agreed well with those obtained with GEOS-Chem (Fig.
560 S3). The annual mean BC levels at the Arctic surface obtained by Flexpart and GEOS-Chem
561 simulations were 48 and 70 ng m⁻³, respectively; the high-altitude values simulated by
562 Flexpart and GEOS-Chem were 35 and 38 ng m⁻³, respectively. The magnitude difference
563 between the BC levels at the Arctic surface could be related to meteorology. ECMWF ERA-
564 Interim data were used as the input for the Flexpart simulation, whereas the GEOS-Chem
565 simulation was driven by assimilated meteorological data from the Goddard Earth
566 Observation System (GEOS-5).

567 The treatments of the BC removal processes could also lead to different simulation
568 results, depending on the model. In terms of BC loss processes, dry and wet depositions
569 were the removal pathways, depending on the particle size and density, in Flexpart. The
570 treatment of meteorology, especially cloud water and precipitation, would therefore affect

Deleted: -

Deleted: 5

Deleted: 6

574 the uncertainties of the simulations. In Flexpart version 10.1, BC particles are separately
575 parameterized as ice nuclei for ice clouds, cloud condensation nuclei for liquid-water clouds,
576 and 90 % as cloud condensation nuclei for mixed-phase clouds. The separation of mixed-
577 phase clouds is realistic, as 77 % of in-cloud scavenging processes occurred in the mixed
578 phase over a 90 day period starting from December 2006 (Grythe et al., 2017).

579 In GEOS-Chem simulations, the BC aging was parameterized based on the number
580 concentration of OH radicals (Liu et al., 2011). The BC was assumed to be hydrophilic in
581 liquid clouds ($T \geq 258$ K) and hydrophobic when serving as ice nuclei in ice clouds ($T < 258$ K)
582 (Wang et al., 2011), with modifications because the scavenging rate of hydrophobic BC was
583 reduced to 5 % of water-soluble aerosols for liquid clouds (Bourgeois and Bey, 2011). Such a
584 treatment is expected to improve the simulation accuracy (Ikeda et al., 2017).

585 In Lagrangian models, the trajectories of particles are computed by following the
586 movement of air masses with no numerical diffusion, although some artificial numerical
587 errors could be generated from stochastic differential equations (Ramli and Esler, 2016). As
588 a result, long-range transport processes can be well simulated (Stohl, 2006; Stohl et al.,
589 2013). In comparison, Eulerian chemical transport models such as GEOS-Chem have the
590 advantage of simulating non-linear processes on the global scale, which enables treatment
591 of the BC aging processes (coating with soluble components) (Bey et al, 2001; Eastham et
592 al., 2018). However, with GEOS-Chem, the capture of intercontinental pollution plumes is
593 difficult because of numerical plume dissipation (Rastigejev et al., 2010). Nevertheless, the
594 agreement between the Flexpart and GEO-Chem simulations of BC source contributions
595 indicates improved reliability of evaluated source contributions to Arctic BC.

596 **4 Conclusions**

597 The source contributions to Arctic BC were investigated by using a Flexpart (version 10.1)
598 transport model that incorporated emission inventories. Flexpart-simulated BC data agreed
599 well with observations at Arctic sites, i.e., Barrow, Alert, Zeppelin, and Tiksi. The source
600 regions and source sectors of BC at the surface and high altitudes (~ 5000 m) over a wide
601 region in the Arctic north of 66° N were simulated. BC at the Arctic surface was sensitive to
602 local emissions and those from nearby Nordic countries (>60° N). These results emphasize
603 the role of anthropogenic emissions such as gas flaring and development of the Northern
604 Sea Route in affecting air quality and climate change in the Arctic. Anthropogenic emissions
605 in the northern regions of Russia were the main source (56 %) of Arctic surface BC annually.
606 In contrast, BC in the Arctic at high altitudes was sensitive to mid-latitude emissions (30–60°
607 N). Although they are geospatially far from the Arctic, anthropogenic emissions in East Asia
608 made a notable (40 %) contribution to BC in the Arctic at high altitudes annually. [Open](#)
609 [biomass](#) burning emissions, which were mainly from Siberia, Alaska, and Canada, were
610 important in summer, contributing 56–85 % of BC at the Arctic surface, and 40–72 % at
611 Arctic high altitudes. Future increases in wildfires as a result of global warming could
612 therefore increase the air pollution level during the Arctic summer. This study clarifies the
613 source regions and sectors of BC in the Arctic. This information is fundamental for
614 understanding and tackling air pollution and climate change in the region.

615
616 *Data Availability.* The data set for simulated footprint and BC source contributions is
617 available on request to the corresponding author.

618
619 *Author contributions.* CZ and YK designed the study. CZ, MT, and IP optimized the Flexpart
620 model. CZ performed Flexpart model simulations, conducted analyses, and wrote the

Deleted: Biomass

Deleted: -

623 manuscript. KI and HT provided data for GEOS-Chem simulations and site observations. All
 624 authors made comments that improved the paper.

625

626 *Competing interests.* The authors declare that they have no conflict of interest.

627

628 *Financial Support.* This study was supported by the Environmental Research and Technology
 629 Development Fund (2-1505) of the Ministry of the Environment, Japan.

630

631 *Acknowledgment.* We acknowledge staffs from the following university and agencies for BC
 632 observational data: Barrow and Tiksi sites are operated by National Oceanic and
 633 Atmospheric Administration; Zeppelin site is operated by Stockholm University; and Alert
 634 site is operated by Environment and Climate Change Canada. We are grateful to two
 635 anonymous reviewers for the comments. We thank Helen McPherson, PhD, from Edanz
 636 Group (www.edanzediting.com/ac) for editing a draft of this manuscript.

Formatted: Font: Not Italic

Formatted: Font: Not Italic

Formatted: Font: Not Italic

Formatted: Font: Italic

637

638 **References**

639 AMAP Assessment 2015: Black carbon and ozone as Arctic climate forcers, Arctic Monitoring
 640 and Assessment Programme (AMAP), Oslo, Norway, 2015.

641 Bey, I., Jacob, D. J., Yantosca, R. M., Logan, J. A., Field, B. D., Fiore, A. M., Li, Q. B., Liu, H. G.
 642 Y., Mickley, L. J., and Schultz, M. G.: Global modeling of tropospheric chemistry with
 643 assimilated meteorology: Model description and evaluation, *J Geophys Res-Atmos*, 106,
 644 23073-23095, doi:10.1029/2001jd000807, 2001.

645 Bourgeois, Q. and Bey, I.: Pollution transport efficiency toward the Arctic: sensitivity to
 646 aerosol scavenging and source regions, *J. Geophys. Res.*, 116, D08213,
 647 doi:10.1029/2010JD015096, 2011.

648 Brock, C. A., Cozic, J., Bahreini, R., Froyd, K. D., Middlebrook, A. M., McComiskey, A.,
 649 Brioude, J., Cooper, O. R., Stohl, A., Aikin, K. C., de Gouw, J. A., Fahey, D. W., Ferrare, R.

650 A., Gao, R. S., Gore, W., Holloway, J. S., Hubler, G., Jefferson, A., Lack, D. A., Lance, S.,
651 Moore, R. H., Murphy, D. M., Nenes, A., Novelli, P. C., Nowak, J. B., Ogren, J. A., Peischl, J.,
652 Pierce, R. B., Pilewskie, P., Quinn, P. K., Ryerson, T. B., Schmidt, K. S., Schwarz, J. P.,
653 Sodemann, H., Spackman, J. R., Stark, H., Thomson, D. S., Thornberry, T., Veres, P., Watts,
654 L. A., Warneke, C., and Wollny, A. G.: Characteristics, sources, and transport of aerosols
655 measured in spring 2008 during the aerosol, radiation, and cloud processes affecting
656 Arctic Climate (ARCPAC) Project, *Atmospheric Chemistry and Physics*, **11**, 2423-2453,
657 doi:10.5194/acp-11-2423-2011, 2011.

658 Cohen, J., Screen, J. A., Furtado, J. C., Barlow, M., Whittleston, D., Coumou, D., Francis, J.,
659 Dethloff, K., Entekhabi, D., Overland, J., and Jones, J.: Recent Arctic amplification and
660 extreme mid-latitude weather, *Nature Geoscience*, **7**, 627-637, doi:10.1038/Ngeo2234,
661 2014.

662 Cozic, J., Verheggen, B., Mertes, S., Connolly, P., Bower, K., Petzold, A., Baltensperger, U.,
663 and Weingartner, E.: Scavenging of black carbon in mixed phase clouds at the high alpine
664 site Jungfraujoch, *Atmos. Chem. Phys.*, **7**, 1797-1807, doi:10.5194/acp-7-1797-2007,
665 2007.

666 Dong, X., Zhu, Q., Fu, J. S., Huang, K., Tan, J., and Tipton, M.: Evaluating recent updated black
667 carbon emissions and revisiting the direct radiative forcing in Arctic, *Geophysical*
668 *Research Letters*, **46**, 3560– 3570. doi:10.1029/2018GL081242, 2019.

669 Eastham, S. D., Long, M. S., Keller, C. A., Lundgren, E., Yantosca, R. M., Zhuang, J. W., Li, C.,
670 Lee, C. J., Yannetti, M., Auer, B. M., Clune, T. L., Kouatchou, J., Putman, W. M., Thompson,
671 M. A., Trayanov, A. L., Molod, A. M., Martin, R. V., and Jacob, D. J.: GEOS-Chem High
672 Performance (GCHP v11-02c): a next-generation implementation of the GEOS-Chem
673 chemical transport model for massively parallel applications, *Geosci Model Dev*, **11**,
674 2941-2953, doi:10.5194/gmd-11-2941-2018, 2018.

675 Eckhardt, S., Quennehen, B., Olivie, D. J. L., Berntsen, T. K., Cherian, R., Christensen, J. H.,
676 Collins, W., Crepinsek, S., Daskalakis, N., Flanner, M., Herber, A., Heyes, C., Hodnebrog,
677 O., Huang, L., Kanakidou, M., Klimont, Z., Langner, J., Law, K. S., Lund, M. T., Mahmood,
678 R., Massling, A., Myriokefalitakis, S., Nielsen, I. E., Nojgaard, J. K., Quaas, J., Quinn, P. K.,
679 Raut, J. C., Rumbold, S. T., Schulz, M., Sharma, S., Skeie, R. B., Skov, H., Uttal, T., von
680 Salzen, K., and Stohl, A.: Current model capabilities for simulating black carbon and
681 sulfate concentrations in the Arctic atmosphere: a multi-model evaluation using a

- 682 comprehensive measurement data set, *Atmospheric Chemistry and Physics*, 15, 9413-
683 9433, doi:10.5194/acp-15-9413-2015, 2015.
- 684 Evangeliou, N., Balkanski, Y., Hao, W. M., Petkov, A., Silverstein, R. P., Corley, R., Nordgren,
685 B. L., Urbanski, S. P., Eckhardt, S., Stohl, A., Tunved, P., Crepinsek, S., Jefferson, A.,
686 Sharma, S., Nojgaard, J. K., and Skov, H.: Wildfires in northern Eurasia affect the budget of
687 black carbon in the Arctic - a 12-year retrospective synopsis (2002-2013), *Atmospheric*
688 *Chemistry and Physics*, 16, 7587-7604, doi:10.5194/acp-16-7587-2016, 2016.
- 689 Evangeliou, N., Kylling, A., Eckhardt, S., Myroniuk, V., Stebel, K., Paugam, R., Zibtsev, S., and
690 Stohl, A.: Open fires in Greenland in summer 2017: transport, deposition and radiative
691 effects of BC, OC and BrC emissions, *Atmospheric Chemistry and Physics*, 19, 1393-1411,
692 doi:10.5194/acp-19-1393-2019, 2019.
- 693 Filimonova, I. V., Komarova, A. V., Eder, L. V., and Provornaya, I. V.: State instruments for the
694 development stimulation of Arctic resources regions, *IOP Conference Series: Earth and*
695 *Environmental Science*, 193, 012069, doi:10.1088/1755-1315/193/1/012069, 2018.
- 696 Garrett, T. J., Brattstrom, S., Sharma, S., Worthy, D. E. J., and Novelli, P.: The role of
697 scavenging in the seasonal transport of black carbon and sulfate to the Arctic,
698 *Geophysical Research Letters*, 38, L16805, doi:10.1029/2011gl048221, 2011.
- 699 Grythe, H., Kristiansen, N. I., Zwaafink, C. D. G., Eckhardt, S., Strom, J., Tunved, P., Krejci, R.,
700 and Stohl, A.: A new aerosol wet removal scheme for the Lagrangian particle model
701 FLEXPART v10, *Geosci Model Dev*, 10, 1447-1466, doi:10.5194/gmd-10-1447-2017, 2017.
- 702 Hegg, D. A., Clarke, A. D., Doherty, S. J., and Ström, J.: Measurements of black carbon
703 aerosol washout ratio on Svalbard, *Tellus B*, 63, 891-900, doi:10.1111/j.1600-
704 0889.2011.00577.x, 2011.
- 705 Hertel, O., Christensen, J. Runge, E. H., Asman, W. A. H., Berkowicz, R., Hovmand, M. F., and
706 Hov, O.: Development and testing of a new variable scale air pollution model – ACDEP,
707 *Atmos. Environ.*, 29, 1267-1290, 1995.
- 708 Hirdman, D., Burkhardt, J. F., Sodemann, H., Eckhardt, S., Jefferson, A., Quinn, P. K., Sharma,
709 S., Strom, J., and Stohl, A.: Long-term trends of black carbon and sulphate aerosol in the
710 Arctic: changes in atmospheric transport and source region emissions, *Atmospheric*
711 *Chemistry and Physics*, 10, 9351-9368, doi:10.5194/acp-10-9351-2010, 2010.
- 712 Huang, K., and Fu, J. S.: A global gas flaring black carbon emission rate dataset from 1994 to
713 2012, *Scientific Data*, 3, 160104. doi:10.1038/sdata.2016.104, 2016.

- 714 Huang, K., Fu, J. S., Prikhodko, V. Y., Storey, J. M., Romanov, A., Hodson, E. L., Cresko, J.,
715 Morozova, I., Ignatieva, Y., and Cabaniss, J.: Russian anthropogenic black carbon:
716 Emission reconstruction and Arctic black carbon simulation, *J Geophys Res-Atmos*, **120**,
717 11306-11333, doi:10.1002/2015jd023358, 2015.
- 718 Ikeda, K., Tanimoto, H., Sugita, T., Akiyoshi, H., Kanaya, Y., Zhu, C. M., and Taketani, F.:
719 Tagged tracer simulations of black carbon in the Arctic: transport, source contributions,
720 and budget, *Atmospheric Chemistry and Physics*, **17**, 10515-10533, doi:10.5194/acp-17-
721 10515-2017, 2017.
- 722 Janssens-Maenhout, G., Crippa, M., Guizzardi, D., Dentener, F., Muntean, M., Pouliot, G.,
723 Keating, T., Zhang, Q., Kurokawa, J., Wankmüller, R., Denier van der Gon, H., Kuenen, J. J.
724 P., Klimont, Z., Frost, G., Darras, S., Koffi, B., and Li, M.: HTAP_v2.2: a mosaic of regional
725 and global emission grid maps for 2008 and 2010 to study hemispheric transport of air
726 pollution, *Atmos. Chem. Phys.*, **15**, 11411–11432, doi:10.5194/acp-15-11411-2015, 2015.
- 727 Keegan, K. M., Albert, M. R., McConnell, J. R., and Baker, I.: Climate change and forest fires
728 synergistically drive widespread melt events of the Greenland Ice Sheet, *P Natl Acad Sci*
729 *USA*, **111**, 7964-7967, doi:10.1073/pnas.1405397111, 2014.
- 730 Kipling, Z., Stier, P., Schwarz, J. P., Perring, A. E., Spackman, J. R., Mann, G. W., Johnson, C.
731 E., and Telford, P. J.: Constraints on aerosol processes in climate models from vertically-
732 resolved aircraft observations of black carbon, *Atmos. Chem. Phys.*, **13**, 5969–5986,
733 doi:10.5194/acp-13-5969-2013, 2013.
- 734 Kirchstetter, T. W., Novakov, T., and Hobbs, P. V.: Evidence that the spectral dependence of
735 light absorption by aerosols is affected by organic carbon, *J Geophys Res-Atmos*, **109**,
736 D21208, doi:10.1029/2004jd004999, 2004.
- 737 [Klimont, Z., Kupiainen, K., Heyes, C., Purohit, P., Cofala, J., Rafaj, P., Borcen-Kleefeld, J., and](#)
738 [Schöpp, W.: Global anthropogenic emissions of particulate matter including black carbon,](#)
739 [Atmos. Chem. Phys., 17, 8681–8723, doi:10.5194/acp-17- 8681-2017, 2017.](#)
- 740 Klonecki, A., Hess, P., Emmons, L., Smith, L., Orlando, J., and Blake, D.: Seasonal changes in
741 the transport of pollutants into the Arctic troposphere-model study, *J Geophys Res-*
742 *Atmos*, **108**, 8367, doi:10.1029/2002jd002199, 2003.
- 743 Koch, D., and Hansen, J.: Distant origins of Arctic black carbon: A Goddard Institute for Space
744 Studies ModelE experiment, *J Geophys Res-Atmos*, **110**, D04204,
745 doi:10.1029/2004jd005296, 2005.

Deleted: -

- 747 [Koch, D., Schmidt, G. A., and Field, C. V.: Sulfur, sea salt, and radionuclide aerosols in GISS](#)
 748 [ModelE, *J. Geophys. Res.*, **111**, D06206, doi:10.1029/2004jd005550, 2006.](#)
- 749 Lack, D. A., and Langridge, J. M.: On the attribution of black and brown carbon light
 750 absorption using the Angstrom exponent, *Atmospheric Chemistry and Physics*, **13**,
 751 10535–10543, doi:10.5194/acp-13-10535-2013, 2013.
- 752 Law, K. S., and Stohl, A.: Arctic air pollution: Origins and impacts, *Science*, **315**, 1537–1540,
 753 doi:10.1126/science.1137695, 2007.
- 754 Liu, J., Fan, S., Horowitz, L. W., and Levy II, H.: Evaluation of factors controlling long-range
 755 transport of black carbon to the Arctic, *J. Geophys. Res.*, **116**, D00A14,
 756 doi:10.1029/2010JD015145, 2011.
- 757 Liu, D., Quennehen, B., Darbyshire, E., Allan, J. D., Williams, P. I., Taylor, J. W., Bauguitte, S. J.
 758 B., Flynn, M. J., Lowe, D., Gallagher, M. W., Bower, K. N., Choulaton, T. W., and Coe, H.:
 759 The importance of Asia as a source of black carbon to the European Arctic during
 760 springtime 2013, *Atmospheric Chemistry and Physics*, **15**, 11537–11555, doi:10.5194/acp-
 761 15-11537-2015, 2015.
- 762 Ma, P.-L., Rasch, P. J., Wang, H., Zhang, K., Easter, R. C., Tilmes, S., Fast, J. D., Liu, X., Yoon, J.-
 763 H., and Lamarque, J.-F.: The role of circulation features on black carbon transport into the
 764 Arctic in the Community Atmosphere Model version 5 (CAM5), *J. Geophys. Res.-Atmos.*,
 765 **118**, 4657–4669, doi:10.1002/jgrd.50411, 2013.
- 766 [McMahon, T. A. and Denison, P. J.: Empirical atmospheric deposition parameters – a survey,](#)
 767 [Atmos. Environ., **13**, 571–585, doi:10.1016/0004-6981\(79\)90186-0, 1979.](#)
- 768 Najafi, M. R., Zwiers, F. W., and Gillett, N. P.: Attribution of Arctic temperature change to
 769 greenhouse-gas and aerosol influences, *Nature Climate Change*, **5**, 246-249,
 770 doi:10.1038/Nclimate2524, 2015.
- 771 Park, R. J., Jacob, D. J., Palmer, P. I., Clarke, A. D., Weber, R. J., Zondlo, M. A., Eisele, F. L.,
 772 Bandy, A. R., Thornton, D. C., Sachse, G. W., and Bond, T. C.: Export efficiency of black
 773 carbon aerosol in continental outflow: Global implications, *J Geophys Res-Atmos*, **110**,
 774 D11205, doi:10.1029/2004jd005432, 2005.
- 775 Qi, L., Li, Q. B., Henze, D. K., Tseng, H. L., and He, C. L.: Sources of springtime surface black
 776 carbon in the Arctic: an adjoint analysis for April 2008, *Atmospheric Chemistry and*
 777 *Physics*, **17**, 9697–9716, doi:10.5194/acp-17-9697-2017, 2017.

Deleted: ¶

Deleted: -

Deleted: -

Deleted: -

Deleted: -

- 783 Quinn, P. K., Bates, T. S., Baum, E., Doubleday, N., Fiore, A. M., Flanner, M., Fridlind, A.,
 784 Garrett, T. J., Koch, D., Menon, S., Shindell, D., Stohl, A., and Warren, S. G.: Short-lived
 785 pollutants in the Arctic: their climate impact and possible mitigation strategies,
 786 *Atmospheric Chemistry and Physics*, 8, 1723–1735, doi:10.5194/acp-8-1723-2008, 2008.
- 787 Ramli, H. M. and Esler, J. G.: Quantitative evaluation of numerical integration schemes for
 788 Lagrangian particle dispersion models, *Geosci. Model Dev.*, 9, 2441–2457,
 789 doi:10.5194/gmd-9-2441-2016, 2016.
- 790 Rastigejev, Y., Park, R., Brenner, M., and Jacob, D.: Resolving intercontinental pollution
 791 plumes in global models of atmospheric transport, *J. Geophys. Res.*, 115, D02302,
 792 doi:10.1029/2009JD012568, 2010.
- 793 Roiger, A., Thomas, J. L., Schlager, H., Law, K. S., Kim, J., Schafler, A., Weinzierl, B.,
 794 Dahlokter, F., Krisch, I., Marelle, L., Minikin, A., Raut, J. C., Reiter, A., Rose, M., Scheibe,
 795 M., Stock, P., Baumann, R., Bouapar, I., Clerbaux, C., George, M., Onishi, I., and Flemming,
 796 J.: Quantifying emerging local anthropogenic emissions in the Arctic region: The ACCESS
 797 aircraft campaign experiment, *B. Am. Meteorol. Soc.*, 96, 441–460, doi:10.1175/Bams-D-
 798 13-00169.1, 2015.
- 799 Sand, M., Berntsen, T. K., von Salzen, K., Flanner, M. G., Langner, J., and Victor, D. G.:
 800 Response of Arctic temperature to changes in emissions of short-lived climate forcers,
 801 *Nature Climate Change*, 6, 286–289, doi:10.1038/Nclimate2880, 2016.
- 802 Schacht, J., Heinold, B., Quaas, J., Backman, J., Cherian, R., Ehrlich, A., Herber, A., Huang, W.
 803 T. K., Kondo, Y., Massling, A., Sinha, P. R., Weinzierl, B., Zanutta, M., and Tegen, I.: The
 804 importance of the representation of air pollution emissions for the modeled distribution
 805 and radiative effects of black carbon in the Arctic, *Atmos. Chem. Phys.*, 19, 11159–11183,
 806 doi:10.5194/acp-19-11159-2019, 2019.
- 807 Schmale, J., Arnold, S. R., Law, K. S., Thorp, T., Anenberg, S., Simpson, W. R., Mao, J., and
 808 Pratt, K. A.: Local Arctic Air Pollution: A Neglected but Serious Problem, *Earths Future*, 6,
 809 1385–1412, doi:10.1029/2018ef000952, 2018.
- 810 Schulz, H., Zanutta, M., Bozem, H., Leaitch, W. R., Herber, A. B., Burkart, J., Willis, M. D.,
 811 Kunkel, D., Hoor, P. M., Abbatt, J. P. D., and Gerdes, R.: High Arctic aircraft measurements
 812 characterising black carbon vertical variability in spring and summer, *Atmospheric
 813 Chemistry and Physics*, 19, 2361–2384, doi:10.5194/acp-19-2361-2019, 2019.

Deleted: -

Deleted: -

Deleted: -

Deleted: -

Deleted: -

- 819 Sharma, S., Leaitch, W. R., Huang, L., Veber, D., Kolonjari, F., Zhang, W., Hanna, S. J.,
820 Bertram, A. K., and Ogren, J. A.: An evaluation of three methods for measuring black
821 carbon in Alert, Canada, *Atmospheric Chemistry and Physics*, 17, 15225–15243,
822 doi:10.5194/acp-17-15225-2017, 2017.
- 823 Shaw, G. E.: The arctic haze phenomenon, *B Am Meteorol Soc*, 76, 2403–2413, 1995.
- 824 Shen, Z. Y., Ming, Y., Horowitz, L. W., Ramaswamy, V., and Lin, M. Y.: On the seasonality of
825 Arctic black carbon, *J. Climate*, 30, 4429–4441, doi:10.1175/Jcli-D-16-0580.1, 2017.
- 826 Shindell, D. T., Chin, M., Dentener, F., Doherty, R. M., Faluvegi, G., Fiore, A. M., Hess, P.,
827 Koch, D. M., MacKenzie, I. A., Sanderson, M. G., Schultz, M. G., Schulz, M., Stevenson, D.
828 S., Teich, H., Textor, C., Wild, O., Bergmann, D. J., Bey, I., Bian, H., Cuvelier, C., Duncan, B.
829 N., Folberth, G., Horowitz, L. W., Jonson, J., Kaminski, J. W., Marmer, E., Park, R., Pringle,
830 K. J., Schroeder, S., Szopa, S., Takemura, T., Zeng, G., Keating, T. J., and Zuber, A.: A multi-
831 model assessment of pollution transport to the Arctic, *Atmos. Chem. Phys.*, 8, 5353–5372,
832 doi:10.5194/acp-8-5353-2008, 2008.
- 833 Sinha, P. R., Kondo, Y., Koike, M., Ogren, J. A., Jefferson, A., Barrett, T. E., Sheesley, R. J.,
834 Ohata, S., Moteki, N., Coe, H., Liu, D., Irwin, M., Tunved, P., Quinn, P. K., and Zhao, Y.:
835 Evaluation of ground-based black carbon measurements by filter-based photometers at
836 two Arctic sites, *J Geophys Res-Atmos*, 122, 3544–3572, doi:10.1002/2016jd025843,
837 2017.
- 838 Stohl, A., Forster, C., Frank, A., Seibert, P., and Wotawa, G.: Technical note: The Lagrangian
839 particle dispersion model FLEXPART version 6.2, *Atmos. Chem. Phys.*, 5, 2461–2474,
840 doi:10.5194/acp-5-2461-2005, 2005.
- 841 Stohl, A.: Characteristics of atmospheric transport into the Arctic troposphere, *J Geophys*
842 *Res-Atmos*, 111, D11306, doi:10.1029/2005jd006888, 2006.
- 843 Stohl, A., Hittenberger, M., and Wotawa, G.: Validation of the Lagrangian particle dispersion
844 model FLEXPART against large-scale tracer experiment data, *Atmos Environ*, 32, 4245-
845 4264, doi:10.1016/S1352-2310(98)00184-8, 1998.
- 846 Stohl, A., Klimont, Z., Eckhardt, S., Kupiainen, K., Shevchenko, V. P., Kopeikin, V. M., and
847 Novigatsky, A. N.: Black carbon in the Arctic: the underestimated role of gas flaring and
848 residential combustion emissions, *Atmospheric Chemistry and Physics*, 13, 8833–8855,
849 doi:10.5194/acp-13-8833-2013, 2013.

Deleted: -

Deleted: -

Deleted: -

Deleted: Atmospheric Chemistry and Physics

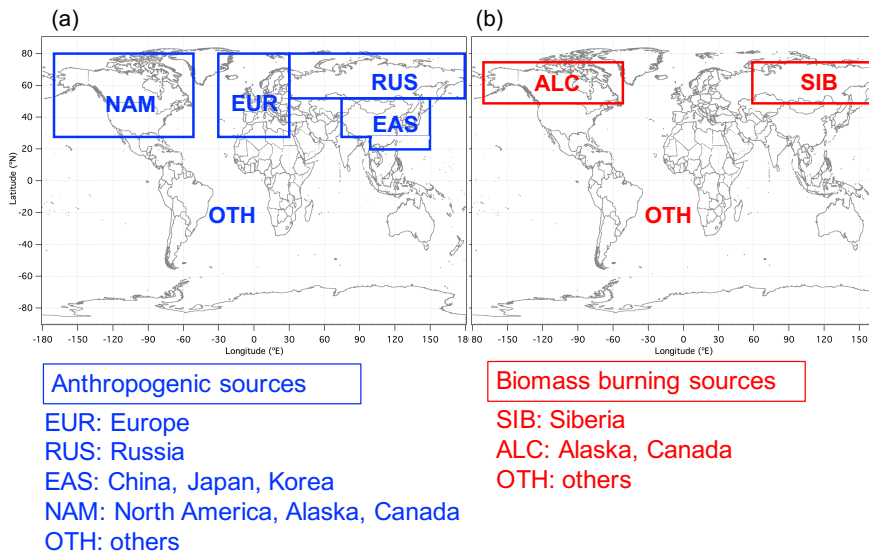
- 854 Taketani, F., Miyakawa, T., Takashima, H., Komazaki, Y., Pan, X., Kanaya, Y., and Inoue, J.:
855 Shipborne observations of atmospheric black carbon aerosol particles over the Arctic
856 Ocean, Bering Sea, and North Pacific Ocean during September 2014, *J Geophys Res-*
857 *Atmos*, 121, 1914-1921, doi:10.1002/2015jd023648, 2016.
- 858 Tietze, K., Riedi, J., Stohl, A., and Garrett, T. J.: Space-based evaluation of interactions
859 between aerosols and low-level Arctic clouds during the Spring and Summer of 2008,
860 *Atmospheric Chemistry and Physics*, 11, 3359-3373, doi:10.5194/acp-11-3359-2011,
861 2011.
- 862 Tilling, R. L., Ridout, A., Shepherd, A., and Wingham, D. J.: Increased Arctic sea ice volume
863 after anomalously low melting in 2013, *Nature Geoscience*, 8, 643-646,
864 doi:10.1038/Ngeo2489, 2015.
- 865 [Tørseth, K., Aas, W., Breivik, K., Fjærraa, A. M., Fiebig, M., Hjellbrekke, A. G., Lund Myhre, C.,
866 Solberg, S., and Yttri, K. E.: Introduction to the European Monitoring and Evaluation
867 Programme \(EMEP\) and observed atmospheric composition change during 1972–2009,
868 *Atmos. Chem. Phys.*, 12, 5447–5481, doi:10.5194/acp-12-5447-2012, 2012.](#)
- 869 Trusel, L. D., Das, S. B., Osman, M. B., Evans, M. J., Smith, B., Fettweis, X., McConnell, J. R.,
870 Noel, B. P. Y., and van den Broeke, M. R.: Nonlinear rise in Greenland runoff in response
871 to post-industrial Arctic warming, *Nature*, 564, 104-108, doi:10.1038/s41586-018-0752-4,
872 2018.
- 873 van der Werf, G. R., Randerson, J. T., Giglio, L., Collatz, G. J., Mu, M., Kasibhatla, P. S.,
874 Morton, D. C., DeFries, R. S., Jin, Y., and van Leeuwen, T. T.: Global fire emissions and the
875 contribution of deforestation, savanna, forest, agricultural, and peat fires (1997–2009),
876 *Atmospheric Chemistry and Physics*, 10, 11707-11735, doi:10.5194/acp-10-11707-2010,
877 2010.
- 878 Veira, A., Lasslop, G., and Kloster, S.: Wildfires in a warmer climate: Emission fluxes,
879 emission heights, and black carbon concentrations in 2090-2099, *J Geophys Res-Atmos*,
880 121, 3195-3223, doi:10.1002/2015jd024142, 2016.
- 881 Wang, H., Rasch, P. J., Easter, R. C., Singh, B., Zhang, R., Ma, P. L., Qian, Y., and Beagley, N.:
882 Using an explicit emission tagging method in global modeling of source-receptor
883 relationships for black carbon in the Arctic: Variations, Sources and Transport pathways,
884 *J. Geophys. Res.-Atmos.*, 119, 12888–12909, doi:10.1002/2014JD022297, 2014.

- 885 Wang, Q., Jacob, D. J., Fisher, J. A., Mao, J., Leibensperger, E. M., Carouge, C. C., Le Sager, P.,
886 Kondo, Y., Jimenez, J. L., Cubison, M. J., and Doherty, S. J.: Sources of carbonaceous
887 aerosols and deposited black carbon in the Arctic in winter-spring: implications for
888 radiative forcing, *Atmos. Chem. Phys.*, **11**, 12453–12473, doi:10.5194/acp-11-12453-
889 2011, 2011.
- 890 Wang, Q., Jacob, D. J., Spackman, J. R., Perring, A. E., Schwarz, J. P., Moteki, N., Marais, E. A.,
891 Ge, C., Wang, J., and Barrett, S. R. H.: Global budget and radiative forcing of black carbon
892 aerosol: constraints from pole-to-pole (HIPPO) observations across the Pacific, *J.*
893 *Geophys. Res. Atmos.*, **119**, 195–206, doi:10.1002/2013JD020824, 2014.
- 894 Winiger, P., Andersson, A., Eckhardt, S., Stohl, A., and Gustafsson, O.: The sources of
895 atmospheric black carbon at a European gateway to the Arctic, *Nat Commun*, **7**, 12776,
896 doi:10.1038/ncomms12776, 2016.
- 897 Winiger, P., Barrett, T. E., Sheesley, R. J., Huang, L., Sharma, S., Barrie, L. A., Yttri, K. E.,
898 Evangeliou, N., Eckhardt, S., Stohl, A., Klimont, Z., Heyes, C., Semiletov, I. P., Dudarev, O.
899 V., Charkin, A., Shakhova, N., Holmstrand, H., Andersson, A., and Gustafsson, O.: Source
900 apportionment of circum-Arctic atmospheric black carbon from isotopes and modeling,
901 *Sci Adv*, **5**, eaau8052, doi:10.1126/sciadv.aau8052, 2019.
- 902 Xu, J. W., Martin, R. V., Morrow, A., Sharma, S., Huang, L., Leaitch, W. R., Burkart, J., Schulz,
903 H., Zanatta, M., Willis, M. D., Henze, D. K., Lee, C. J., Herber, A. B., and Abbatt, J. P. D.:
904 Source attribution of Arctic black carbon constrained by aircraft and surface
905 measurements, *Atmospheric Chemistry and Physics*, **17**, 11971-11989, doi:10.5194/acp-
906 17-11971-2017, 2017.
- 907 Yu, K., Keller, C. A., Jacob, D. J., Molod, A. M., Eastham, S. D., and Long, M. S.: Errors and
908 improvements in the use of archived meteorological data for chemical transport
909 modeling: an analysis using GEOS-Chem v11-01 driven by GEOS-5 meteorology, *Geosci*
910 *Model Dev*, **11**, 305-319, doi:10.5194/gmd-11-305-2018, 2018.
- 911 Zhu, C., Kobayashi, H., Kanaya, Y., and Saito, M.: Size-dependent validation of MODIS
912 MCD64A1 burned area over six vegetation types in boreal Eurasia: Large underestimation
913 in croplands, *Scientific reports*, **7**, 4181, doi:10.1038/s41598-017-03739-0, 2017.

Table 1. Comparison of BC source contributions in the Arctic surface

<u>Model and versions</u>	<u>Model type</u>	<u>Wet-deposition</u>	<u>Grid resolution</u>	<u>Meteorology</u>	<u>Emissions</u>	<u>Domain/Sites</u>	<u>Year/season</u>	<u>Major source regions/sectors</u>
<u>Flexpart-WRF 6.2</u>	<u>Lagrangian</u>	<u>Stohl et al. (2005)</u>	<u>unspecified</u>	<u>WRF forecast</u>	<u>ECLIPSE, FINN</u>	<u>continental Norway and Svalbard</u>	<u>spring 2013</u>	<u>Asian anthropogenic</u>
<u>Flexpart 6.2</u>	<u>Lagrangian</u>	<u>Stohl et al. (2005)</u>	<u>1° × 1°</u>	<u>ECMWF operational</u>	<u>Unspecified (BC sensitivities were calculated)</u>	<u>Alert, Barrow, Zeppelin</u>	<u>1989-2009</u>	<u>Northern Eurasia</u>
<u>Flexpart 6.2</u>	<u>Lagrangian</u>	<u>Stohl et al. (2005)</u>	<u>1° × 1°</u>	<u>ECMWF operational</u>	<u>ECLIPSE4(GAINS), GFED3</u>	<u>Arctic (north of 66°N)</u>	<u>2008-2010</u>	<u>Flaring (42%), residential (>20%)</u>
<u>Flexpart 9.2</u>	<u>Lagrangian</u>	<u>Stohl et al. (2005)</u>	<u>1° × 1°</u>	<u>ECMWF operational</u>	<u>ECLIPSE5(GAINS), GFED4.1</u>	<u>Arctic (north of 66.7°N)</u>	<u>2011-2015</u>	<u>Residential and open burning (39%)</u>
<u>Flexpart 10.1</u>	<u>Lagrangian</u>	<u>Grythe et al. (2017)</u>	<u>1° × 1°</u>	<u>ECMWF operational</u>	<u>HTAP2, GFED3, Huang et al. (2015) for Russia flaring</u>	<u>Arctic (north of 66°N)</u>	<u>2010</u>	<u>Flaring (36%), open burning (18%), residential (15%), others (31%)</u>
<u>GEOS-Chem 9.02</u>	<u>CTM</u>	<u>Wang et al. (2011)</u>	<u>2° × 2.5°</u>	<u>GEOS-5</u>	<u>HTAP2, GFED3, Huang et al. (2015) for Russia flaring</u>	<u>Arctic (north of 66°N)</u>	<u>2007-2011</u>	<u>Russia (62%)</u>
<u>GEOS-Chem</u>	<u>CTM</u>	<u>Wang et al. (2011)</u>	<u>2° × 2.5°</u>	<u>GEOS-5</u>	<u>Bond et al. (2004), Zhang et al. (2009), GFED3</u>	<u>Alert, Barrow, Zeppelin</u>	<u>April 2008</u>	<u>Asian anthropogenic (35–45%), Siberian biomass burning (46–64%)</u>
<u>GEOS-Chem</u>	<u>CTM</u>	<u>Wang et al. (2011)</u>	<u>2° × 2.5°</u>	<u>GEOS-5</u>	<u>Bond et al. (2007), FLAMBE</u>	<u>North America Arctic</u>	<u>April 2008</u>	<u>Open fire (50%)</u>

<u>GEOS-Chem10.01</u>	<u>CTM</u>	<u>Wang et al. (2011)</u>	<u>2° x 2.5°</u>	<u>GEOS-5</u>	<u>HTAP2, ECLIPSE5, GFED4</u>	<u>Alert, Barrow, Zeppelin, Arctic (north of 66.5°N)</u>	<u>2009-2011</u>	<u>N-Asian anthropogenic (40-45%) in winter-spring</u>	<u>Xu et al. (2017)</u>	Formatted: Font: (Default) Calibri
<u>GISS ModelE</u>	<u>GCM</u>	<u>Koch et al. (2006)</u>	<u>4° x 5°</u>	<u>Internal</u>	<u>Bond et al. (2004), Cooke and Wilson (1996)</u>	<u>Arctic (north of ~60°N)</u>	<u>Annual general</u>	<u>South Asia</u>	<u>Koch and Hanse (2005)</u>	Formatted: Font: (Default) Calibri

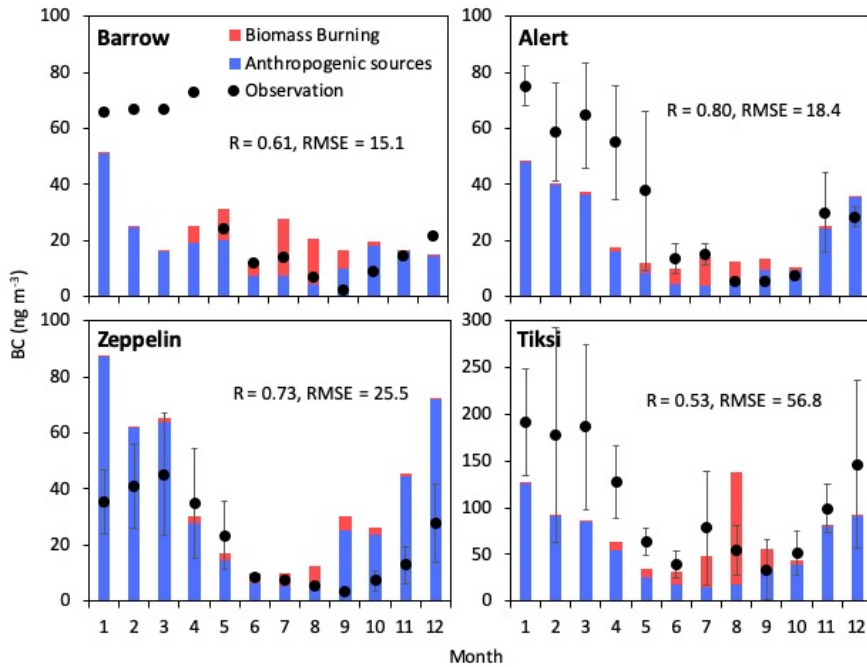


915
916 Figure 1. Regional separation for quantification of BC in the Arctic from (a) anthropogenic
917 and (b) open biomass burning sources.
918

Deleted: -----Page Break-----

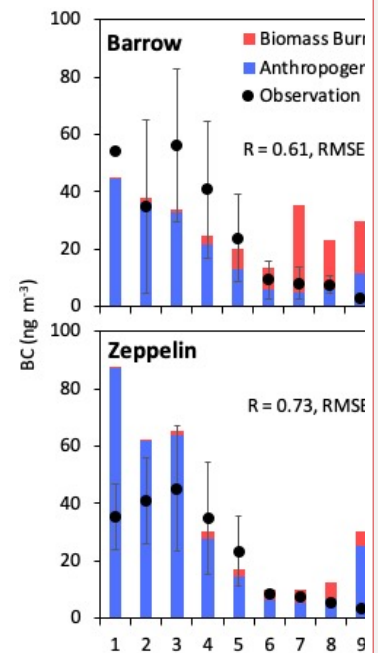
1

Deleted: -



922
 923 Figure 2. Observed (filled circles) and modeled (bars) seasonal variations in BC mass
 924 concentrations at Arctic sites. Contributions from anthropogenic sources (blue) and [open](#)
 925 [biomass](#) burning (red) in each month are shown. Monthly averages of observed (filled
 926 circles) and simulated (bars) BC were conducted for 2007–2011 at Alert, Canada (62.3° W,
 927 82.5° N), and Zeppelin, Norway (11.9° E, 78.9° N), [for 2009 at Barrow, USA \(156.6° W, 71.3°](#)
 928 [N\)](#), and for 2010–2014 at Tiksi, Russia (128.9° E, 71.6° N). *R* and RMSE indicate correlation
 929 coefficient and root-mean-square error (ng m^{-3}), respectively.

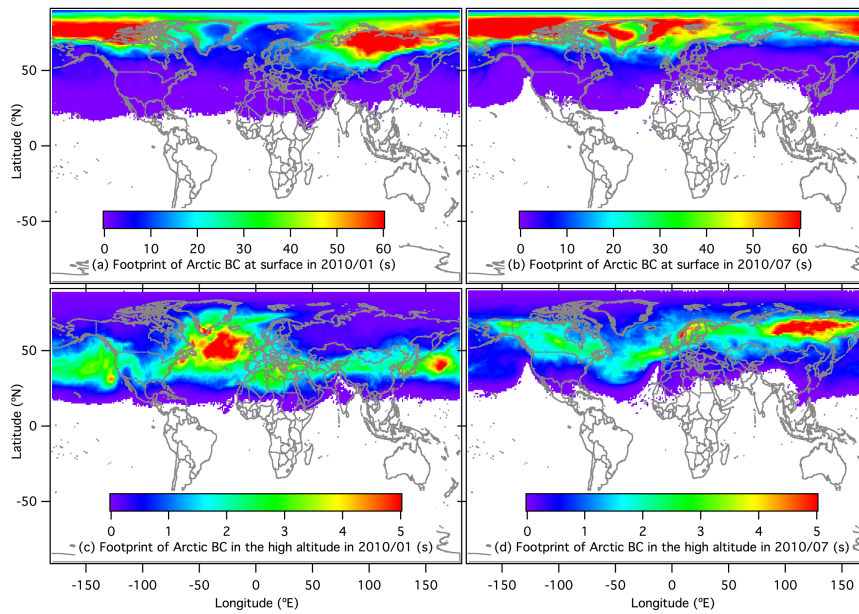
930



Deleted:

Deleted: biomass

Deleted: Barrow, USA (156.6° W, 71.3° N),



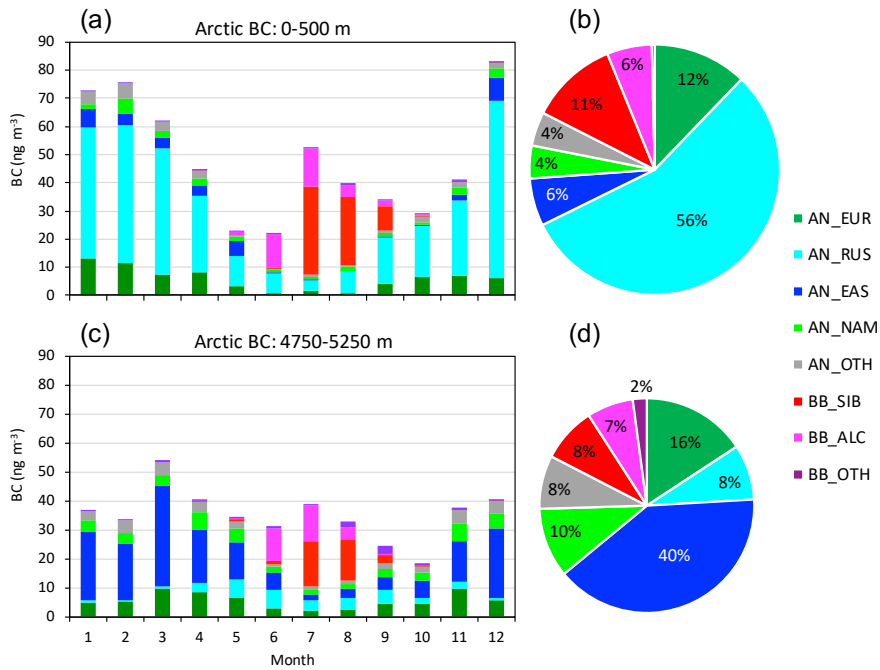
934

935 Figure 3. Footprints of Arctic BC shown as retention time(s) of (a) BC at surface (0–500 m) in

936 January 2010, (b) BC at surface in July 2010, (c) BC at high altitudes (4750–5250 m) in

937 January 2010, and (d) BC at high altitudes (4750–5250 m) in July 2010.

938

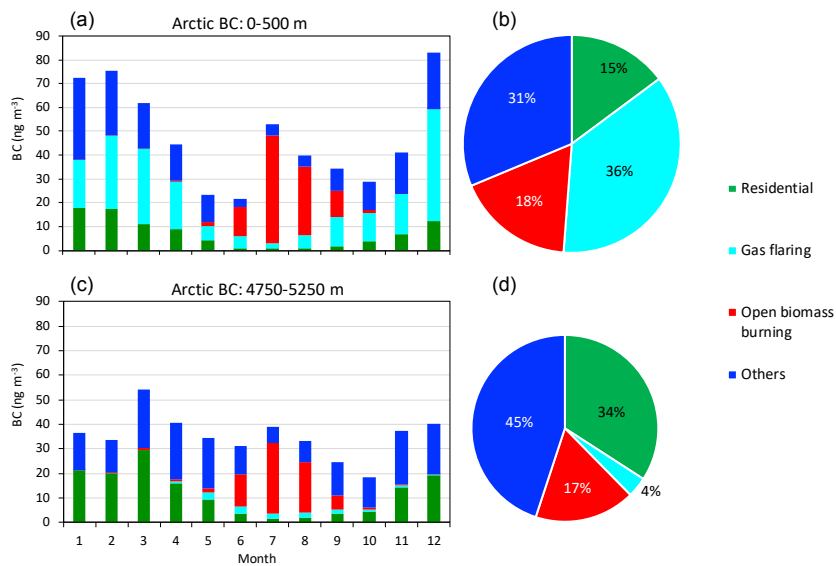


939

940 Figure 4. Contributions of anthropogenic sources and open biomass burning from each
 941 region to (a) seasonal variations in Arctic surface BC, (b) annual mean Arctic surface BC, (c)
 942 seasonal variations in Arctic BC at high altitudes, and (d) annual mean of Arctic BC at high
 943 altitudes.

944

Deleted: biomass

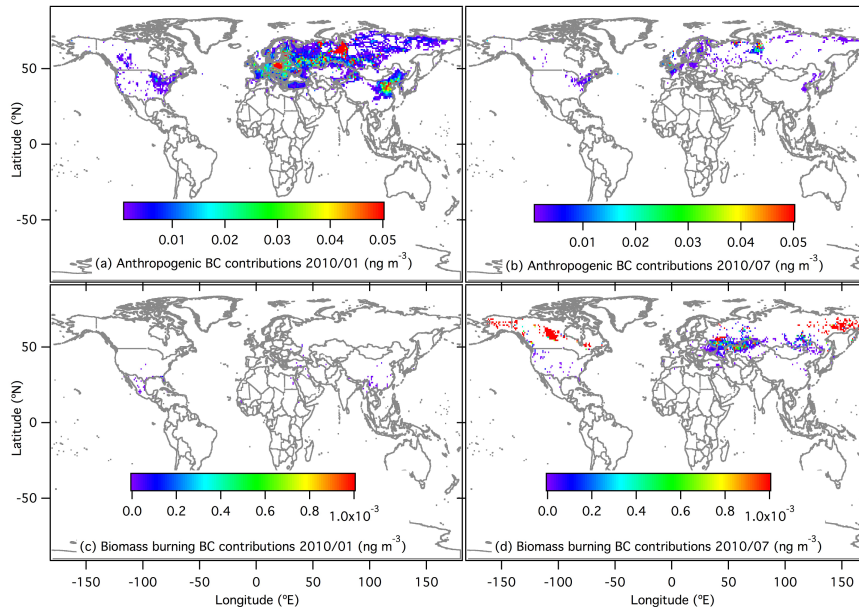


946

947 Figure 5. Sectorial contributions from residential combustion (including fossil fuel and
 948 biofuel combustions), gas flaring, open biomass burning and others (energy other than gas
 949 flaring, industry and transport) to (a) seasonal variations in Arctic surface BC, (b) annual
 950 mean Arctic surface BC, (c) seasonal variations in Arctic BC at high altitudes, and (d) annual
 951 mean of Arctic BC at high altitudes.

952

Deleted: ¶



954

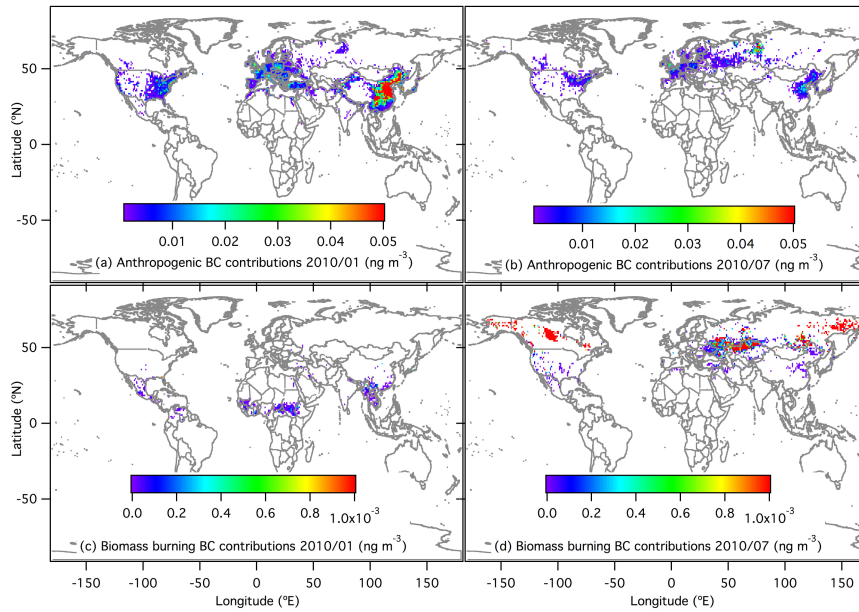
955 Figure 6. Spatial distributions of contributions to Arctic BC at surface (0–500 m) for (a)
 956 anthropogenic contributions in January 2010, (b) anthropogenic contributions in July 2010,
 957 (c) **open** biomass burning contributions in January 2010, and (d) **open** biomass burning
 958 contributions in July 2010.

959

Deleted: 5

Deleted: -

Deleted: -



963

964 Figure 7. Spatial distributions of contributions to Arctic BC at high altitudes (4750–5250 m)

965 for (a) anthropogenic contributions in January 2010, (b) anthropogenic contributions in July

966 2010, (c) **open** biomass burning contributions in January 2010, and (d) **open** biomass967 **burning** contributions in July 2010.

968

Deleted: 6

Deleted: -

Deleted: -

972 Supplementary materials for

973 **Flexpart v10.1 simulation of source contributions to Arctic black carbon**

974 Chunmao Zhu¹, Yugo Kanaya^{1,2}, Masayuki Takigawa^{1,2}, Kohei Ikeda³, Hiroshi Tanimoto³,

975 Fumikazu Taketani^{1,2}, Takuma Miyakawa^{1,2}, Hideki Kobayashi^{1,2}, Ignacio Pissso⁴

976

977 ¹Research Institute for Global Change, Japan Agency for Marine–Earth Science and
978 Technology (JAMSTEC), Yokohama 2360001, Japan

979 ²Institute of Arctic Climate and Environmental Research, Japan Agency for Marine–Earth
980 Science and Technology, Yokohama 2360001, Japan

981 ³National Institute for Environmental Studies, Tsukuba 305-8506, Japan

982 ⁴NILU – Norwegian Institute for Air Research, Kjeller 2027, Norway

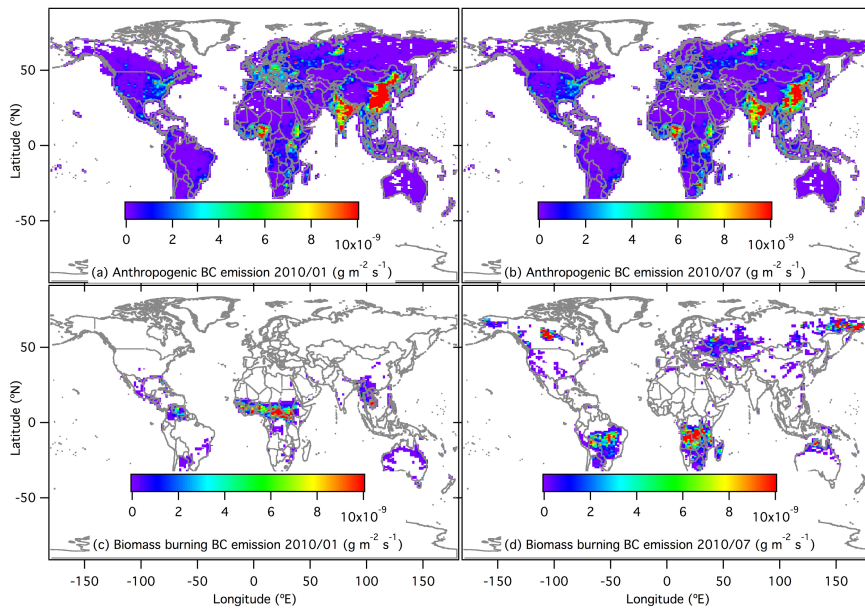
983

984 Correspondence to Chunmao Zhu (chmzhu@jamstec.go.jp)

985

986

987 This file contains Figures S1, Figure S2, and Figure S3.



988

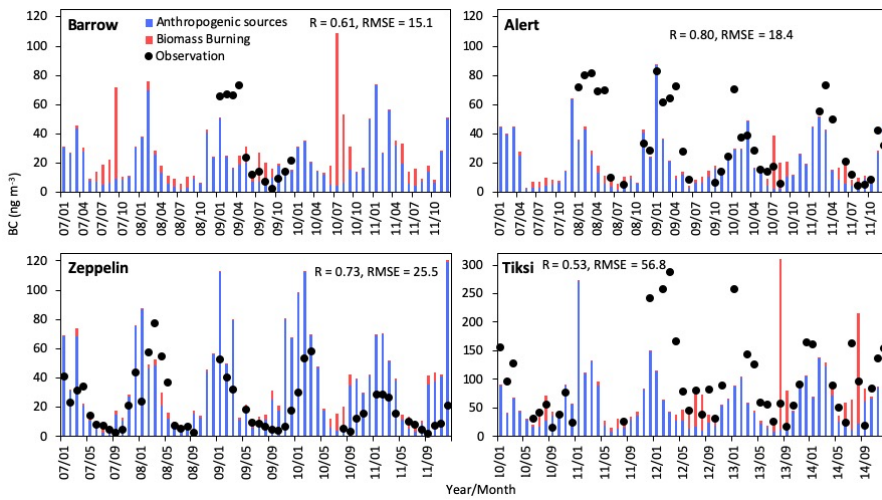
989 Figure S1. Spatial distributions of BC emissions from (a) anthropogenic sources in January

990 2010, (b) anthropogenic sources in July 2010, (c) open biomass burning in January 2010, and991 (d) open biomass burning in July 2010.

992

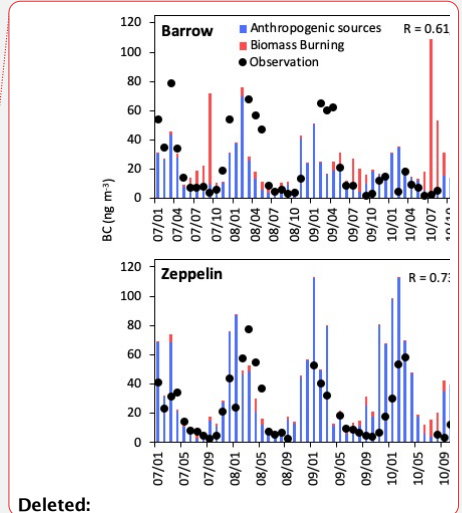
Deleted: biomass

Deleted: biomass



995

996 Figure S2. Time series of observed (filled circles) and modeled (bars) seasonal variations in BC
 997 mass concentrations at Arctic sites. Contributions from anthropogenic sources (blue) and open
 998 biomass burning (red) in each month are shown. Monthly averages of observed (filled circles)
 999 BC are shown for 2007–2011 at Alert, Canada (62.3° W, 82.5° N), and Zeppelin, Norway (11.9°
 1000 E, 78.9° N), for 2009 at Barrow, USA (156.6° W, 71.3° N), and for 2010–2014 at Tiksi, Russia
 1001 (128.9° E, 71.6° N). R and RMSE indicate correlation coefficient and root-mean-square error
 1002 (ng m⁻³), respectively.
 1003

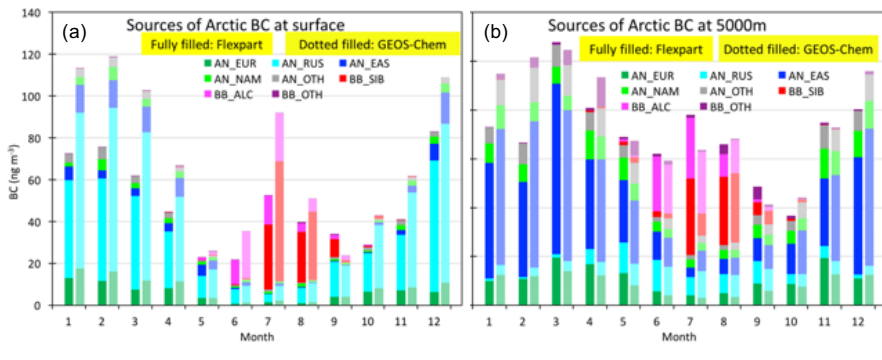


Deleted:

Deleted:

Deleted: and simulated (bars)

Deleted: Barrow, USA (156.6° W, 71.3° N),



1008

1009 Figure S3. Comparison of Flexpart-simulated Arctic BC sources with those obtained by using
 1010 GEOS-Chem.

1011

Page 11: [1] Deleted	Zhu Chunmao	11/29/19 11:25:00 AM
----------------------	-------------	----------------------

Page 11: [2] Deleted	Zhu Chunmao	11/28/19 10:31:00 AM
----------------------	-------------	----------------------